

Type I' and Real Algebraic Geometry

Freddy Alexander Cachazo and Cumrun Vafa

Jefferson Physical Laboratory

Harvard University

Cambridge, MA 02138

Abstract

We revisit the duality between type I' and heterotic strings in 9 dimensions. We resolve a puzzle about the validity of type I' perturbation theory and show that there are regions in moduli which are not within the reach of type I' perturbation theory. We find however, that all regions of moduli are described by a special class of real elliptic $K3$'s in the limit where the $K3$ shrinks to a one dimensional interval. We find a precise map between the geometry of dilaton and branes of type I' on the one hand and the geometry of real elliptic $K3$ on the other. We also argue more generally that strong coupling limits of string compactifications generically do not have a weakly coupled dual in terms of any known theory (as is exemplified by the strong coupling limit of heterotic strings in 9 dimensions for certain range of parameters).

1. Introduction

Thanks to the discovery of duality symmetries in string theory we now understand in many cases what the light degrees of freedom in a string theory are in various regimes of coupling constant and compactification geometry of string theory. In this way one has been able to connect various theories to each other in an unexpected way. In many cases this leads to a unified picture of string theory suggesting there is a unique underlying theory with different manifestations in various regimes, unifying Type IIA, B, type I, heterotic and 11 dimensional M-theory, in a single framework.

Indeed, in the case of maximal number of supersymmetries ($N = 32$) in various dimensions, Witten raised the following question [1] : If we consider strong coupling regime of type II strings compactified on tori, then in principle we can discover new consistent theories. It was very surprising that by considering various limits leaving at least 4 non-compact spacetime dimensions [1] one ended up with a theory which had a simple description in terms of compactifications of known string theories or 11 dimensional supergravity, M-theory. In other words a consequence of [1] was the discovery of a single new 11 dimensional M-theory, which together with other string theories in the case of maximal number of supersymmetries gives a complete description of all boundaries of moduli space of theories with $N = 32$ supercharges.

However this leaves open the possibility that if we consider other cases, for example compactifications with less supersymmetry, we may discover new theories by considering their strong coupling limit. In fact an example of this situation was discovered in [2] where by considering heterotic string compactified on T^2 one ended up in the strong coupling regime with a theory which did not have a well defined description in terms of a single string theory. The new theory, F-theory, put together various (p, q) type IIB strings which are non-perturbative relative to each other in a single compactification. It involved using (p, q) 7-branes of type IIB taking advantage of the non-perturbative U-duality group of type IIB, namely the $SL(2, \mathbf{Z})$. The question raised was to come up with a complete low energy description of this new theory.

The geometry of branes was encoded in terms of a limit of elliptic $K3$ manifold suggesting a 12 dimensional origin. However it is clear that a formulation in 12 dimension must involve some new constructions (including the lack of 12 dimensional Poincare invariance) which, despite some progress, is still an open question. The problem becomes acute when one considers compactifications of F-theory with less supersymmetry. For example to determine even the massless degrees of freedom of F-theory on elliptic Calabi-Yau threefold,

one has to appeal to various consistency conditions (including anomaly cancellations in the chiral 6-dimensional theory) to predict the spectrum [3]. This clearly is unsatisfactory and one would like to have a more direct approach in finding the light degrees of freedom. Thus the new theory discovered is more mysterious than superstring theories or M-theory.

The fact that different limits of various other string compactification may exist which have no interpretation in terms of M-theory, String theories, or F-theory, was already pointed out in [4] where it was suggested that the strong coupling limit of asymmetric orbifold compactifications of string theory [5] would provide such examples. In fact many interesting such examples have been constructed in [6] which in strong coupling regimes may define new theories. One can also use U-dualities in the form of an orbifold to construct F-theory like theories which in many cases correspond to new theories [4] which do not have any conventional known dual analog. Various other F-theory like theories which correspond to various specific $K3$ geometric duals has also been considered which correspond to new theories [7][8][9].

To obtain limits which have no interpretation in terms of M-theory or string theories, one can also use conventional compactification geometries. For example even with $N = 32$ supercharges, it was shown in [10] that if we consider toroidal compactification leaving 2 or less non-compactified dimensions similar thing happens.

In fact there are more such examples involving compactification to 4 dimensions. Consider Type IIA string theory compactified on Calabi-Yau threefolds. Let us assume that the threefold is neither elliptically fibered, nor $K3$ fibered. Let us consider the limit of strong coupling of this theory fixing the volume of Calabi-Yau in string frame¹. Then we do not have a candidate for a dual theory. In fact if there is a dual theory description involving known theories, this will be a new duality which cannot be related to other known dualities using adiabatic principle. This is because all the known dualities will involve $K3$ or elliptic compactifications. In particular the known duality of type IIA on Calabi-Yau threefolds and heterotic on $K3 \times T^2$ [11] (see also [12]) goes through $K3$ or elliptic fibered Calabi-Yau manifolds [13] and this can be related to string dualities in 6 dimensions using the adiabatic principle [14]. Thus it is likely that for each Calabi-Yau threefold which is not elliptic or $K3$ fibered, we end up defining a new theory by considering a strong coupling limit of type IIA compactification. Given that in some sense the generic Calabi-Yau threefold is not elliptic or $K3$ fibered [15] we would conclude that “most” type II

¹ In terms of M-theory this corresponds to compactification on a large circle times a Calabi-Yau threefold with infinitesimal volume.

compactifications with $N = 2$ supersymmetries in $4d$ have strong coupling limits involving presumably unknown theories.

It is thus apparent that the unifying framework to consider all string theories will have various unrecognizable corners in the moduli space of various compactifications in addition to the ones already known. The main aim of the present paper is to consider one such corner. This is the compactification of heterotic strings on a circle. The parameters characterizing this compactification, in addition to heterotic string coupling constant, involve the radius of the circle and the sixteen parameters specifying the expectation value of Wilson loops around the circle. For certain regions of moduli at strong coupling limit of heterotic string there is a dual description in terms of type I' theory [16] on an interval related to the Type I–heterotic ($SO(32)$) duality in 10 dimensions [1]. We will show that for specific choices of Wilson loop variables and radii, in the strong coupling limit there is no perturbative Type I' description. Moreover we show that, just as in the case of F-theory, all regimes of parameters can be usefully characterized by the geometry of a particular class of *real* elliptic rational $K3$ surface, as was anticipated in [3]. We will also see that this real $K3$, has a natural and precise relation with the geometry of dilaton and branes of type I'.

The organization of this paper is as follows: In section 2 we review the theories dual to heterotic strings in 10, 9 and 8 dimensions. In section 3 we discuss a puzzle in the case of type I' dual of heterotic string in 9 dimensions. In section 4 we discuss global aspects of moduli of type I' (or heterotic) theory in 9 dimensions. In section 5 we resolve the puzzles raised in section 3, and indicate why the regime of validity of type I' perturbation theory misses some regions of moduli space. In section 6 we consider the limit of F-theory corresponding to decompactifying one circle and show how the relevant limit is captured by a particular type of real elliptic $K3$'s. In section 7 we discuss how real elliptic $K3$'s fills the gap in moduli space where the type I' perturbation breaks down. In particular we recover extra branes postulated by Morrison and Seiberg [17] predicted from duality with heterotic strings. In section 8 we give various explicit examples. Finally some details of the computations are presented in appendices A and B.

2. Heterotic dual theories in 10, 9 and 8 dimensions Reviewed

In 10 dimensions there are two inequivalent heterotic theories, one with $SO(32)$ gauge group and the other with $E_8 \times E_8$. The strong coupling limit of the former has a complete

description in terms of the weak coupling limit of Type I theory [1]. However, the latter does not have a conventional string theory as its strong coupling limit but is instead dual to a compactification of M-theory on S^1/Z_2 [18].

When we go down in dimensions compactifying on T^k we find that both heterotic theories can be connected continuously, i.e., they belong to the same moduli space. This is due to the uniqueness of Lorentzian self-dual lattices [19].

Strong coupling limit of heterotic strings in the 9 dimensional case follows from compactifying the 10 dimensional duality between heterotic $Spin(32)/Z_2$ and Type I on an S^1 . In this case, if we study the heterotic theory at strong coupling and radius close to the critical radius we end up with Type I' (which is T-dual to Type I).

In 8 dimensions, the heterotic dual description is given in terms of F-theory compactified on an elliptic $K3$ surface. This captures the Type IIB compactification on P^1 with 24 (p,q) 7-branes. It is natural to ask about the connection between the 8 dimensional description and the 9 dimensional one. In particular one would like to take the large radius limit of the 8 dimensional dual theories and see what one ends up in 9 dimensions.

It is the aim of this section to review the known descriptions of these theories in 8,9 and 10 dimensions and develop the necessary relations that will be useful in the rest of this work.

2.1. 10 and 9 Dimensions

Let us start by considering the 10 dimensional low energy effective actions in the string frame for the heterotic $Spin(32)/Z_2$ and Type I theories. Since these two theories have $N = 1$ supersymmetry and the same gauge group, the two actions should just be related by a field redefinition.

For the heterotic string we have,

$$S_{het} = \int d^{10}x \sqrt{-g_h} e^{-2\phi_h} [R_h + \partial_\mu \phi \partial^\mu \phi - |H_3|^2 - Tr_v(|F_2^2|)] \quad (2.1)$$

and using the following field redefinition,

$$g_{I\mu\nu} = e^{-\phi_h} g_{h\mu\nu} \quad \phi_I = -\phi_h \quad F_3 = H_3 \quad A_{I1} = A_{h1} \quad (2.2)$$

we get the Type I effective action,

$$S_I = \int d^{10}x \sqrt{-g_I} e^{-2\phi_I} [R_I + \partial_\mu \phi \partial^\mu \phi - |F_3|^2] - \int e^{-\phi_I} Tr_v(|F_2^2|) \quad (2.3)$$

Compactifying on a circle the 10 dimensional duality should give us information about the heterotic strong coupling limit in 9 dimensions, and in fact, for big enough heterotic radius this is the case. Nevertheless one of the most interesting features of the heterotic string is the enhancement of the gauge symmetries at some points in the moduli space where the radius is not much larger than the string length. Using the above field redefinitions we can see that

$$\lambda_h^{10} = \frac{1}{\lambda_I^{10}} \quad R_I = \frac{R_h}{(\lambda_h^{10})^{1/2}} \quad (2.4)$$

Therefore for strongly coupled heterotic string $\lambda_h^{10} \gg 1$ and $R_h^2 \simeq R_{hc}^2 = 2(1 - A^2/2)$, where R_{hc} is the critical radius², at which point new massless gauge bosons appear, we get $R_I \ll 1$. This implies that we need to perform a T-duality in order to understand the physics clearly. The theory thus obtained is called the Type I'.

In general, we can think about Type I as a theory in ten dimensions containing one orientifold 9-plane and 32 D9-branes. When we compactify on a circle and perform a T-duality we get a type IIA theory on S^1/Z_2 with two orientifold 8-planes located at the fixed points of the Z_2 action and 16 D-8 branes at generic positions on the interval. At a generic point in the moduli space we have an $U(1)^{18}$ gauge group. Where $U(1)^{16}$ corresponds to the positions of the branes, one $U(1)$ from the graviphoton and the last $U(1)$ is related to the R-R one form. Using the fact that when (n) D-branes are on the top of each other we get an $U(n)$ enhancement of the gauge group and if in addition they are located at one of the orientifolds we get $SO(2n)$, it is easy to see that $SO(32)$ and all its regular subalgebras can be obtained in this fashion³.

The map between the moduli spaces of heterotic strings and type I' was worked out in [16] for certain regions of parameter space which we will now review. In the heterotic theory we have the 16 Wilson lines $\theta^I, I = 1, \dots, 16$, the radius R_h and the coupling constant $\Lambda_h = e^{\phi_h}$. On the Type I' side we have the 16 positions of the branes $x^I, I = 1 \dots 16$, where x stands for the coordinate along the interval and runs from 0 to 2π , B and C that control the behavior of the type I' dilaton at the orientifolds and the physical length of the interval respectively.

² The value of the Regge slope for the heterotic $SO(32)$ is taken to be $\alpha'_h = 2$

³ The information about all possible gauge symmetries allowed in heterotic strings is nicely encoded in the extended Dynkin diagram of $SO(32)$ as we will discuss it in detail in section 4.

It turns out to be convenient to define the following function,

$$z(x) = \frac{3}{\sqrt{2}}(B + 8x_{cm} - \frac{1}{2} \sum_{I=1}^{16} |x - x_I|) \quad (2.5)$$

where $x_{cm} = \frac{1}{16} \sum x_I$ is the position of the center of mass of the 16 D-8 branes. The metric in string frame is given by, $g_{MN} = \Omega^2(x)\eta_{MN}$, and the dilaton of Type I' are given by,

$$e^{\phi_{I'}} = (Cz(x))^{-5/6}, \quad \Omega(x) = C^{5/6}z(x)^{-1/6} \quad (2.6)$$

Before writing down the explicit map between the heterotic and Type I' moduli, let us express the Type I' dilaton as a function not of the coordinate distance x but of the proper distance measured from the orientifold at $x = 0$.

Let us call $\phi(\bar{x})$ the proper distance from $x = 0$ to $x = \bar{x}$. This is given by,

$$\phi(\bar{x}) = \frac{5}{2^{3/2}} \int_0^{\bar{x}} \Omega(y) dy \quad (2.7)$$

where the numerical factor was introduced for later convenience.

Let us define $\frac{1}{g(\phi)} = e^{-\phi_{I'}}$ to be the coupling, ϕ_I to be the position of the I^{th} brane in the interval and $\frac{1}{g_0} = (CB)^{5/6}$ to be the coupling at the orientifold at $x = 0$. The final answer is given by

$$\frac{1}{g(\phi)} = \frac{1}{g_0} + 8\phi_{cm} - \frac{1}{2} \sum_{I=1}^{16} |\phi - \phi_I|. \quad (2.8)$$

Let us now go back to the map of the moduli spaces between $SO(32)$ heterotic string and type I'. The map was obtained in [16] by comparing the gravitational and gauge actions, the mass of a K-K heterotic state and its corresponding dual type I' winding state. The heterotic radius is given by,

$$R_h = 2^{-3/4} \left(\int_0^{2\pi} dx z(x)^{1/3} \right)^{1/2} \left(\int_0^{2\pi} dx z(x)^{-1/3} \right)^{-1} \quad (2.9)$$

and the heterotic dilaton up to a numerical multiplicative constant⁴ is

$$e^{2\phi_h} = C^{10/3} \left(\int_0^{2\pi} dx z(x)^{1/3} \right)^3 \left(\int_0^{2\pi} dx z(x)^{-1/3} \right)^{-1} \quad (2.10)$$

⁴ The constant contains some factors of $\alpha'_{I'}$.

Finally, the Wilson lines and the positions of the branes can be related by computing the mass of off-diagonal vector boson. Let $A = (\theta_1, \dots, \theta_{16})$ be the Wilson lines, then,

$$\theta_I = \frac{1}{2} \left(\int_0^{x^I} dx z(x)^{-1/3} \right) \left(\int_0^{2\pi} dx z(x)^{-1/3} \right)^{-1} \quad (2.11)$$

It is easy to see that for generic x^I and B , the strong coupling limit of the heterotic strings, i.e. $\lambda_h \gg 1$, can be obtained by taking $C \gg 1$. Moreover, the map allows us to compute R_h and θ_I only from B and x^I .

Let us consider two examples that will be useful to illustrate how the map works and how Type I' avoids possible contradictions at the points where the heterotic is getting enhanced gauge symmetries.

Consider first the following set of Wilson lines $A = (0^n, (\frac{1}{2})^{16-n})$ that was studied in [16]. This corresponds to having n D8-branes at $x = 0$ and $16 - n$ D8-branes at $x = 2\pi$. Using (2.9) we get,

$$R_h = \frac{1}{2}(8-n)^{1/2} \frac{[(B + 2\pi(8-n))^{4/3} - B^{4/3}]^{1/2}}{[(B + 2\pi(8-n))^{2/3} - B^{2/3}]} \quad (2.12)$$

and from (2.6) the type I' dilaton is,

$$e^{\phi_{I'}} = [B + (8-n)x_9]^{-5/6} \quad (2.13)$$

As mentioned before, the behavior of the dilaton at $x = 0$ is controlled by B and in particular it blows up for $B = 0$. This is usually a sign that something interesting should be happening on the dual heterotic theory. For $B = 0$ we have,

$$e^{\phi_{I'}} \sim x_9^{-5/6} \quad R_h = \frac{1}{2}|n-8|^{1/2} \quad (2.14)$$

But $R_h = \frac{1}{2}|n-8|^{1/2}$ is precisely the critical radius of the heterotic string for the given Wilson line, i.e., $R_c^2 = 2(1 - A^2/2)$. The gauge group enhancements in each case are listed in the Table 1.

n	G_o	R_c^2	$G_{enhanced}$
7	$SO(14) \times U(1)$	1/4	E_8
6	$SO(12) \times U(1)$	1/2	E_7
5	$SO(10) \times U(1)$	3/4	E_6
4	$SO(8) \times U(1)$	1	$E_5 \simeq SO(10)$
3	$SO(6) \times U(1)$	5/4	$E_4 \simeq SU(5)$
2	$SO(4) \times U(1)$	3/2	$E_3 \simeq SU(3) \times SU(2)$
1	$SO(2) \times U(1)$	7/4	$E_2 \simeq SU(2) \times U(1)$
0	$U(1)$	2	$E_1 \simeq SU(2)$

Table 1: Gauge groups G_o at generic radius corresponding to Wilson lines of the form $A = (0^n, (\frac{1}{2})^{16-n})$. Enhanced gauge groups $G_{enhanced}$ at the critical radius $R_c^2 = \frac{1}{4}|n - 8|$.

Therefore, we see that perturbation theory breaks down avoiding the contradiction of having new massless states on the heterotic side that are not in the perturbative spectrum of Type I'. It has been shown that the new massless vector bosons of the heterotic string can be identified with non-perturbative states of Type I'. In particular, we have D0-branes that become massless at the orientifold with infinite coupling [20][21].

The second example is given by the following Wilson line $A = (0^{15}, \lambda)$. This corresponds to 15 D8-branes at $x = 0$ and one brane whose position we denote by x_1 . This is a particular case of the examples studied in [20]. The map is given by,

$$R_h = \frac{1}{\sqrt{2}} \frac{\left(\frac{b^2 - a^2}{7} + \frac{a^2 - c^2}{8}\right)^{1/2}}{\left(\frac{b-a}{7} + \frac{a-c}{8}\right)} \quad \lambda = \frac{1}{2} \frac{\frac{(b-a)}{7}}{\frac{b-a}{7} + \frac{a-c}{8}} \quad (2.15)$$

where $a = (B - 7x_1)^{2/3}$, $b = B^{2/3}$ and $c = (B + x_1 - 16\pi)^{2/3}$.

This configuration for generic x_1 and B has $SO(30)$ as gauge group. However, for special values of x_1 and B enhancements of $SO(30)$ can be obtained. This will be studied in detail in section 5. In particular, for $x_1 = 0$ this is equivalent to the $n = 0$ case of the first example.

$E_8 \times E_8$ from Type I':

Later in the paper we will need a more detailed description for the map between heterotic string at the $E_8 \times E_8$ gauge symmetry enhancement point with the type I' parameters. In the above we discussed how one obtains one extra E_8 symmetry by considering 7 branes on one orientifold with infinite coupling. If we did this on each orientifold we would get $E_8 \times E_8$. In other words consider the following family of Wilson lines $A = (0^7, \frac{1}{2} - \lambda, \lambda, (\frac{1}{2})^7)$ studied in [22]. This corresponds to having 7 D8-branes at $x = 0$, 7 D8-branes at $x = 2\pi$ and two more D8-branes symmetrically located in the interval at positions x_1 and $x_2 = 2\pi - x_1$. This configuration generically corresponds to an unbroken $SO(14) \times SO(14) \times U(1)^4$ gauge group.

The map in this case involves R_h , and λ as functions of B and x^1 and it is given by,

$$R_h = 2^{-3/2} 3^{1/2} \frac{[3(a^4 - b^4) + 4(\pi - x_1)a]^{1/2}}{[3(a^2 - b^2) + 2(\pi - x_1)a^{-1}]} \quad (2.16)$$

where $a = (B + x_1)^{1/3}$ and $b = B^{1/3}$.

And,

$$\lambda = \frac{3}{4} \frac{a^2 - b^2}{[3(a^2 - b^2) + 2(\pi - x_1)a^{-1}]} \quad (2.17)$$

The dilaton behaves as follows,

$$e^{\phi_{I'}} = \begin{cases} (B+x)^{-5/6} & 0 < x < x_1 \\ (B+x_1)^{-5/6} & x_1 < x < x_2 \\ (B+2\pi-x)^{-5/6} & x_2 < x < 2\pi \end{cases} \quad (2.18)$$

It is clear that the $B \rightarrow 0$ limit is also very interesting in this case. Indeed, for $B = 0$ the dilaton blows up at both orientifold points. This is a generic feature whenever the position of the center of mass of the branes is in the middle of the interval, i.e., $x_{cm} = \pi$.

Let us see what the corresponding heterotic behavior is for $B = 0$. From (2.16) and (2.17) we get that,

$$R_h^2 = \frac{3}{8} x_1 \frac{(4\pi - x_1)}{(2\pi + x_1)^2} \quad \lambda = \frac{3}{4} \left[3 + 2 \frac{\pi - x_1}{x_1} \right]^{-1} \quad (2.19)$$

It is easy to invert the second equation and plug $x = x(\lambda)$ in the first to get $R_h^2 = 2\lambda(\frac{1}{2} - \lambda)$ that is precisely the critical radius at which the heterotic string will have an $E_8 \times E_8$ gauge enhancement. Also note that for $x_1 = \pi$ we get $\lambda = \frac{1}{4}$, and two branes in the middle are on top of each other, and that corresponds to an extra $SU(2)$.

For unbroken $E_8 \times E_8$ it is also natural to work with heterotic $E_8 \times E_8$ variables (R_{E8} , $\lambda_{E8} = e^{\phi_{E8}}$) instead of the $SO(32)$ heterotic variables (R_{SO} or λ , $\lambda_{SO} = e^{\phi_{SO}}$) that we have been using, since the Wilson lines in the former are all zero while in the latter they are functions of R_{SO} . The map is worked out in Appendix A with the following results,

$$R_{SO} = \frac{R_{E8}}{(R_{E8}^2 + 2)} \quad \lambda_{E8} = (R_{E8}^2 + 2)^{1/2} \lambda_{SO} \quad (2.20)$$

Now let us use the map from Type I' to the heterotic $SO(32)$ and (2.20) to find the map between the Type I' variables and the $E_8 \times E_8$ heterotic string variable. From (2.19) and (2.20) we get,

$$R_{E8}^2 = \frac{2}{3} \left(\frac{4\pi - x_1}{x_1} \right) \quad \text{or} \quad x_1 = 2\pi \left(\frac{4}{3R_{E8}^2 + 2} \right) \quad (2.21)$$

Using (2.10) we can compute C in terms of R_{E8} and λ_{E8} (remember that in (2.10) $e^{\phi_h} = \lambda_{SO}$) with the following result,

$$C^{5/3} = \lambda_{E8} \frac{(3R_{E8}^2 + 2)^{5/3}}{R_{E8}^3} \quad (2.22)$$

Having done this we are ready to compute all the quantities that will be relevant in section 8.2. The Type I' dilaton is given by,

$$e^{\phi_{I'}} = C^{-5/6} z(x)^{-5/6} = \lambda_{E8}^{-1/2} \frac{R_{E8}^{3/2}}{(3R_{E8}^2 + 2)^{5/6}} z(x)^{-5/6} \quad (2.23)$$

where $z(x) = \frac{3}{\sqrt{2}} [\pi - \frac{1}{2}|x - x_1| - \frac{1}{2}|x - (2\pi - x_1)|]$. This comes from (2.5) by setting $B = 0$ and x_1 is given in (2.21).

The metric is given by,

$$ds^2 = \Omega^2(x) (\eta_{MN} dx^M dx^N) = \lambda_{E8} \frac{(3R_{E8}^2 + 2)^{5/3}}{R_{E8}^3} z(x)^{-1/3} (\eta_{MN} dx^M dx^N) \quad (2.24)$$

Finally we need to compute the proper distances from $x = 0$ to $x = x_1$ and from $x = x_1$ to $x = 2\pi - x_1$.

Let us start with $x = 0$ to $x = x_1$,

$$\Phi_1 = \int_0^{x_1} \Omega(x) dx = \frac{\lambda_{E8}^{1/2}}{R_{E8}^{3/2}} \quad (2.25)$$

and from $x = x_1$ to $x = 2\pi - x_1$,

$$\Phi_2 = \int_{x_1}^{2\pi - x_1} \Omega(x) dx = \lambda_{E8}^{1/2} \frac{(R_{E8}^2 - 2)}{R_{E8}^{3/2}} \quad (2.26)$$

Notice that on the heterotic $E_8 \times E_8$ we are **not** at the critical radius since $E_8 \times E_8$ is not reached by an enhancement of the gauge group. However, the extra $SU(2)$ we mentioned before that is perturbative from Type I' since it corresponds to the two branes in the middle coinciding at $x = \pi$ corresponds according to (2.26) to $R_{E8}^2 = 2$ that is nothing but the critical radius for zero Wilson line.

This concludes our review of the 9 dimensional description using type I'.

2.2. 8 Dimensions

If we try to extend the analysis of the previous section by further compactifying on another S^1 in order to get a description of the strongly coupled heterotic theory in 8 dimensions, it is easy to see that in general we will fail since the two radii of the Type I theory will be small and we will be forced to perform T-duality on both circles. This

implies, for instance, in the case of unbroken $SO(8)^4$, that the Type I' coupling behaves as follows,

$$\lambda_{I'} = \frac{1}{R_{h,1}R_{h,2}} \quad (2.27)$$

therefore if the two heterotic radii are of the order of critical radius then we are out of the perturbative regime of type I'.

The full description of the heterotic moduli space is achieved by considering F-theory compactified on an elliptic K3 [2]. The elliptic fibration over P^1 is given by,

$$y^2 = x^3 + f(z)x + g(z) \quad (2.28)$$

where z is the coordinate over the sphere, $f(z)$ and $g(z)$ are polynomials of degree 8 and 12 respectively.

The discriminant of this equation gives the location of the 24 singular fibers over P^1 and is given by,

$$\Delta = 4f^3(z) + 27g^2(z) \quad (2.29)$$

The complex structure of the fiber located at a point z is given by

$$j(\tau) = 1728 \frac{4f^3(z)}{\Delta} \quad (2.30)$$

where $j(\tau)$ is the invariant modular function. This function can be written as a Laurent series in $q = e^{2\pi i\tau}$ given by,

$$j(\tau) = q^{-1} + 744 + 196884q + 21493760q^2 + \dots \quad (2.31)$$

The F-theory geometry captures the Type IIB compactified on P^1 with 24 (p,q)-7 branes transverse to the P^1 and located at the positions of the singular fibers. The complexified IIB coupling constant $\tau = \chi + ie^{-\phi}$ is identified with the complex structure of the fibers and undergoes $SL(2, \mathbf{Z})$ monodromy. The metric in the Einstein frame for this compactification is given by [23]

$$ds^2 = k \text{Im}(\tau) \left| \frac{\eta^2(\tau)}{\Delta^{1/12}} dz \right|^2 + \eta_{\mu\nu} dx^\mu dx^\nu \quad (2.32)$$

where $\eta(\tau) = q^{1/24} \prod_{n=1}^{\infty} (1 - q^n)$, and k is an overall constant controlling the volume of the sphere.

The last ingredient is the volume of the P^1 that is a positive real number and is identified with the heterotic coupling constant in 8 dimensions. Therefore the strong coupling limit corresponds to a large P^1 and the geometrical picture is a good description.

The possible gauge group on the heterotic side are reproduced on the F-theory by developing ADE singularities on the $K3$. The possible fibers that one can get when two or more singular fibers come to the same point were classified by Kodaira and are given in table 2 together with the order of the zero that $f(z)$, $g(z)$ and Δ should have at those points.

$\text{orf}(f(z))$	$\text{ord}(g(z))$	$\text{ord}(\Delta)$	Fiber Type	Singularity Type
≥ 0	≥ 0	0	smooth	none
0	0	n	I_n	A_{n-1}
≥ 1	1	2	II	none
1	≥ 2	3	III	A_1
≥ 2	2	4	IV	A_2
2	≥ 3	$n+6$	I_n^*	D_{n+4}
≥ 2	3	$n+6$	I_n^*	D_{n+4}
≥ 3	4	8	IV^*	E_6
3	≥ 5	9	III^*	E_7
≥ 4	5	10	II^*	E_8

Table 2: Kodaira classification of singularities of an elliptic $K3$ according to the order of vanishing of $f(z)$, $g(z)$ and $\Delta(z)$.

The precise map between both moduli spaces is in general very complicated, but it is known for several cases in which the IIB coupling τ is constant over the sphere, for example $SO(8)^4$ [24], and for the $E_8 \times E_8$ unbroken point where τ is not constant [3][25]. The map in the case of $E_8 \times E_8$ will be used in section 8 as an example of the limit to 9 dimensions.

3. Puzzles in 9 Dimensions

In the context of Type I', Seiberg studied the theory seen by a D4 brane probe [26] and found evidence for the existence of conformal quantum field theories when the D4 brane probe was placed at the orientifold with infinite coupling. The conformal theory flows to

an $SU(2)$ supersymmetric gauge theory by a deformation, where the $SU(2)$ is the gauge symmetry seen on the probe. That the string coupling be infinite at the orientifold was related to the fact that the conformal theory with $SU(2)$ gauge symmetry on the probe would need to come from a theory with infinite coupling if it has a chance of flowing from a conformal theory, because of simple dimensional analysis of Yang-Mills coupling constant in 5 dimensions. Moreover the quantum field theory one obtains depends on how many D8 branes are placed at the orientifold point. If there are n of them, one obtains an $SU(2)$ gauge theory with n massless hypermultiplets. Furthermore it was suggested that these theories have a global E_{n+1} symmetry. This follows from the fact that the target space has the corresponding gauge symmetry, as reviewed in the previous section, and the gauge symmetry corresponds to global symmetries in the probe theory.

The same critical theories were also obtained in a geometrical context by considering M-theory compactification on Calabi-Yau threefolds, where the threefold has a shrinking 4 dimensional submanifold corresponding to a Del Pezzo surface [27][17]. Del Pezzo surfaces are 2 complex dimensional Kähler manifolds with positive c_1 , and are obtained by considering the blow up of P^2 at up to $m \leq 8$ points, and in addition $P^1 \times P^1$. The isomorphism with the probe picture required identifying the number of blowup points of P^2 , m with $m = n + 1$ where n is the number of D8 branes at the orientifold. However there was a discrepancy between the geometry and the probe picture. Namely for P^2 with no points blown up, there was no brane probe description, as it would correspond to $n = -1$ D8 branes at the orientifold! Moreover for $n = 0$, i.e. infinite coupling at the orientifold plane without any D8 branes present, there were two possible choices for the geometry (rather than one anticipated from type I' probe picture), namely P^2 blown up at one point or $P^1 \times P^1$. The probe in these two cases would have to give an $N = 1$ supersymmetric $SU(2)$ gauge theory with no matter. What distinguishes the two choices is a discrete Z_2 choice of θ angle [27] related to the non-triviality of $\pi_4(SU(2)) = Z_2$. Moreover the two theories are distinguished by the condition that for the case corresponding to $P^1 \times P^1$ there is a global $SU(2)$ symmetry for the conformal theory on the probe, whereas for the case corresponding to P^2 blown up at one point (corresponding to a non-trivial choice of the discrete theta angle), there is no global symmetry on the probe conformal theory.

Type I' perturbation theory should break down as we approach either of these two conformal theories, because they correspond to $1/g = 0$ at the orientifold. But they could be viewed as boundaries of regions where type I' perturbation theory is valid. However, the same cannot be said for the conformal theory associated to P^2 . Not only we do not

have any type I' perturbative brane picture in this regime, the probe gauge theory does not flow to an $SU(2)$ but rather to a $U(1)$. This strongly suggests that there are *regions* (not just boundaries) in the moduli space where type I' perturbation breaks down.

On the other hand aspects of BPS bound states and moduli space for type I' were studied in [21], with emphasis on subloci in moduli space where heterotic string predicts enhanced gauge symmetries. These correspond to codimension one subspaces of moduli space. In other words these loci correspond to “walls” in the moduli space. If these walls decompose the moduli space into disconnected components, then one would argue that Type I' perturbation theory could potentially break down. In other words, the perturbative type I' would describe the interior of only one region in moduli space and the other regions cannot be reached by changing moduli. It was argued in [21] that the domain walls do not decompose the moduli space into disconnected components. This was based on studying some examples, and the general statement was suggested as a conjecture. As we will discuss in the next section, indeed the conjecture is correct and *the moduli space is connected even after removing the walls*.

We thus seem to have two contradictory expectations: Namely the arguments in [21] suggest that type I' perturbation covers the entire moduli space, whereas the probe picture suggests that type I' perturbation should break down beyond some regime of parameters. We will resolve this puzzle in section 5 and show that the completion of regions where type I' perturbation applies does not cover the full moduli space. However before we do this, it is important to have a deeper understanding of the global aspects of moduli space of type I' (or heterotic) theory in 9 dimensions. This is what we turn to in the next section.

4. Global Aspects of Moduli Space in 9 Dimensions

Consider compactification of heterotic string or Type I theory from 10 to 9, on a circle. As discussed before, the moduli space of this theory, in the heterotic language, corresponds to varying the radius of the circle, the 16 Wilson lines and the coupling constant. The total space is

$$\mathcal{M} = \mathbf{R}^+ \times \hat{\mathcal{M}}$$

$$\hat{\mathcal{M}} = SO(17, 1; \mathbf{Z}) \backslash SO(17, 1; \mathbf{R}) / SO(17, R)$$

where R^+ labels the coupling constant of heterotic string and $\hat{\mathcal{M}}$ parameterizes the 17 dimensional space of the radius of the circle and the 16 Wilson lines. The T-duality group is given by $G = SO(17, 1; \mathbf{Z})$.

Before quotienting by G , the 17 dimensional space $SO(17, 1; \mathbf{R})/SO(17, R)$ is simply the 17 dimensional Hyperbolic space, with constant negative curvature. Thus the global aspects of the moduli space are completely encoded by the group G and its action. We will describe the known mathematical aspects of this moduli space [28] as well as connect it to known facts about heterotic string and its moduli. This will in particular lead us to a concrete parametrization of the fundamental domain of the moduli space in terms of heterotic string variables.

The group G is intimately related to a generalized Dynkin diagram:

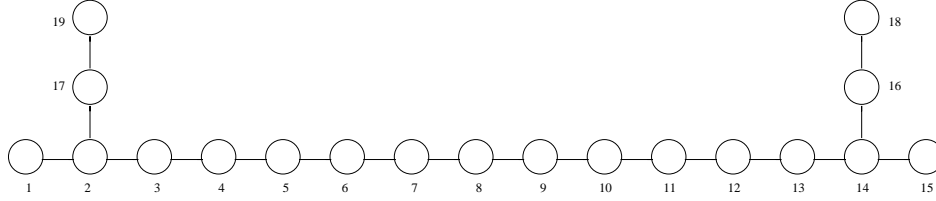


Figure 1: Generalized Dynkin diagram for $\Gamma^{17,1}$. The basis are chosen to show the embedding of the Dynkin diagram of $SO(32)$ explicitly.

The meaning of this diagram is as follows: G is generated by elements labeled by nodes of the diagram, g_i , satisfying

$$g_i^2 = 1$$

Moreover if the corresponding nodes are not connected by a line, then the generators commute

$$g_i g_j = g_j g_i \tag{4.1}$$

and if they are connected one gets the relation

$$(g_i g_j)^3 = 1 \tag{4.2}$$

In addition to get the full group G we need a Z_2 involution which conjugates the generators according to the outer automorphism of the above Dynkin diagram. We will ignore this extra Z_2 in most of this paper and instead consider the double cover of the actual moduli space (in the Type I' description this Z_2 corresponds to exchanging the two ends of the interval, and in the heterotic string description it is the outer automorphism exchanging the two E_8 's).

The elements g_i can be also viewed as Weyl reflections in the Narain lattice $\Gamma^{17,1}$. In particular for each node g_i there is a vector $v_i \in \Gamma^{17,1}$ with the property that

$$v_i^2 = 2$$

(we are choosing the signature on $\Gamma^{17,1}$ corresponding to $(+^{17}, -^1)$) and the Weyl reflection is given as

$$w \rightarrow w - (w \cdot v_i)v_i$$

This clearly is an automorphism of $\Gamma^{17,1}$ (as it preserves the inner product) and so is an element of G . The statement is that G is generated by 19 such Weyl reflections, given by 19 vectors v_i . Moreover, the inner product of these vectors is given by the above extended Dynkin diagram⁵. In particular

$$v_i \cdot v_j = 0 \quad \text{disconnected nodes}$$

$$v_i \cdot v_j = -1 \quad \text{connected nodes}$$

It is easy to check that the Weyl reflections generated by such v_i 's satisfy the relations given in (4.1) and (4.2). In the Narain description of the vector, each v_i corresponds to

$$v_i = (P_L^i, P_R^i)$$

where P_L^i is a 17 dimensional vector and P_R^i is a one dimensional vector, and changing the moduli of the Narain lattice, corresponds to a Lorentz $SO(17,1)$ rotation on the vector. The inner product being given by

$$v_i^2 = (P_L^i)^2 - (P_R^i)^2 = 2$$

If one chooses the Lorentz rotation so that $P_R^i = 0$, this corresponds to an enhanced gauge symmetry, where a $U(1)$ gets promoted to $SU(2)$. Note that this involves one condition, and so it is a 16 dimensional subspace of the 17 dimensional parameter space. In this context the non-trivial Weyl reflection symmetry of $SU(2)$ acts as a Z_2 on the parameters of the theory. The fixed point of this transformation on the Teichmuller space is exactly the locus where we have (at least) an enhanced $SU(2)$ symmetry. This is because at the $SU(2)$ point the Weyl symmetry is a gauge symmetry of the theory and it maps the theory to itself. Let us denote this 16 dimensional subspace by D_i . The D_i divides the 17 dimensional space in two parts mapped to each other by the Z_2 action, which is a symmetry of the theory. One can choose the moduli space to be on one side of D_i . In

⁵ For some aspects of the relation between this extended Dynkin diagram and heterotic strings in 9 dimensions see [29][30].

particular the D_i can be viewed as boundaries of moduli space. The statement that G is generated by Weyl reflection about v_i 's (modulo the Z_2 outer automorphism noted before) implies that all the T-duality symmetries can be understood as Weyl symmetries of some $SU(2)$ at some points on moduli space.

If we consider a collection of N vectors v_i and consider the subspace of the moduli space given by the common intersection locus of the corresponding D_i , this gives a $17 - N$ dimensional subspace. Moreover on this subspace the corresponding $P_R^i = 0$, and the heterotic string will have an enhanced gauge symmetry of rank N whose Dynkin diagram (which may be disconnected) is given by the corresponding nodes. This is clear from the heterotic perspective as the P_L^i 's will form the root lattice of the gauge symmetry group. From this description it is also clear that not all the N loci D_i intersect, otherwise we would get Dynkin diagrams which do not correspond to any group. We thus conclude that the only D_i that have common intersection are the ones for which the corresponding Dynkin nodes is that of an allowed group. This information thus gives us the geometry of intersection of D_i 's. It also tells us all the allowed enhanced gauge symmetries that we can obtain in this case. In particular the maximal gauge symmetry enhancements that we can have would correspond to rank 17 groups whose Dynkin diagram is given by keeping all the nodes of the extended Dynkin diagram of G after deletion of 2 of its nodes.

Now we are ready to describe the moduli space of $\hat{\mathcal{M}}$. The moduli space can be chosen to be very similar to the fundamental domain of $SL(2, \mathbf{Z})$ which is a subspace of the hyperbolic 2-space with three boundaries: two boundaries at $\tau_1 = \pm 1/2$ and the third corresponding to the sphere $\tau_1^2 + \tau_2^2 = 1$. The moduli space for $\hat{\mathcal{M}}$ can be chosen to be given by a subspace of the 17 dimensional hyperbolic space B^{17} with 19 boundaries corresponding to D_i . The geometry resembles that of a higher dimensional chimney (see Fig.2).

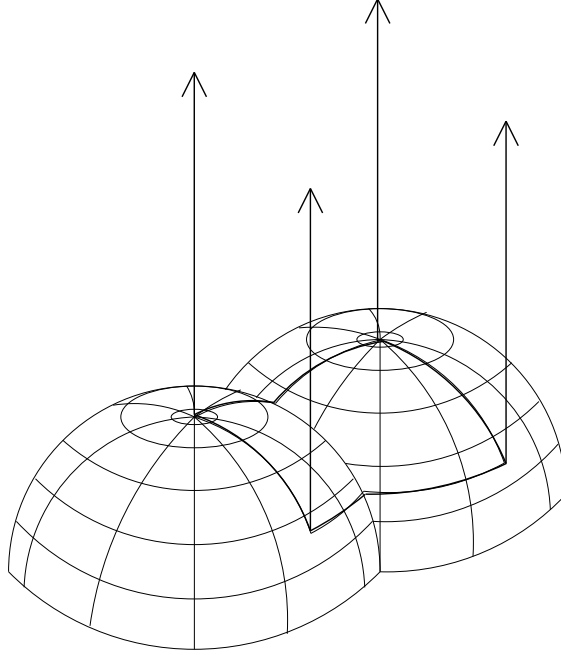


Figure 2: A chimney bounded by two spherical walls on the bottom represents the Moduli Space $\hat{\mathcal{M}}$.

17 of the boundaries, corresponding to the nodes of the affine $SO(32)$ in the extended Dynkin diagram correspond to 17 straight walls of the chimney and two of the boundaries, corresponding to the two extra nodes of the Dynkin diagram correspond to spherical “bottom” of the chimney. The geometry of their intersection is already discussed above and is in accordance with allowed enhanced gauge symmetry points. The direction corresponding to increasing the radius of the 9-th direction of the $SO(32)$ heterotic string is along the linear direction of the chimney. This geometry can be understood relatively simply: Note that the cross section of the chimney (the analog of τ_1 for upper half-plane) is 16 dimensional. Moreover, for large R it should be identified with the Wilson lines for the $SO(32)$ theory. The choices of inequivalent Wilson lines for the $SO(32)$ theory are given by choices of arbitrary 16 vevs θ_i in the Cartan of $SO(32)$ modulo the action of the symmetries. The symmetries in this case are the shifts of θ_i and also the Weyl action. The group they form is the affine Weyl group, and that is why the extended Dynkin diagram of $SO(32)$ enters the moduli space of flat bundles on a circle.⁶ The fundamental domain for the $SO(32)$ Wilson lines are given by the cross section of the chimney enclosed by 17 walls which are in 1-1 correspondence with the nodes of affine $SO(32)$. This describes the

⁶ A similar statement is also true for all other groups.

cross section of the chimney. Let us be more explicit and give a quantitative description of the cross section of this chimney, parametrizing it in R^{16} and identifying each of the boundaries with the respective node in the Dynkin Diagram.

Let $\theta_1, \dots, \theta_{16}$ be coordinates of R^{16} , the $Spin(32)$ wilson line can be chosen to be a diagonal matrix representing the action on the fundamental representation, i.e. $W = \text{diag}(e^{2\pi i \theta_1}, e^{-2\pi i \theta_1}, \dots, e^{2\pi i \theta_{16}}, e^{-2\pi i \theta_{16}})$. Clearly, the Weyl group has as subgroup the permutation group S_{16} , and therefore it is possible to introduce an ordering without loss of generality. Let $0 \leq |\theta_1| \leq |\theta_2| \leq \dots \leq |\theta_{15}| \leq |\theta_{16}| \leq 1$ be the region of R^{16} that would be expanded if no further elements of the Weyl group are considered.

Moreover the Weyl group has more elements generated by $\theta_i \rightarrow -\theta_i$ done for *pairs* of θ_i 's and similiarly for $\theta_i \rightarrow 1 - \theta_i$ for a pair. Therefore we see that the actual choice for the moduli can be chosen to be $0 \leq \theta_2 \leq \dots \leq \theta_{15} \leq \frac{1}{2}$, $|\theta_1| \leq \theta_2$, $\theta_{15} \leq \theta_{16} \leq 1 - \theta_{15}$ (the condition of having even pairs in the above Weyl action is what makes the first and last θ 's have different regimes). Thus, we can see the 17 boundaries defining the 17 codimension 1 walls in R^{16} . There are 13 whenever any $\theta_i = \theta_{i+1}$ for $i = 2, \dots, 14$, the last 4 are given when either θ_1 or θ_{16} meet any of their two boundaries.

Each of the first 13 boundaries given by $\theta_i = \theta_{i+1}$ corresponds to the node labelled by i in the Dynkin diagram of figure 1. The two boundaries given by $\theta_1 = \theta_2$ and $\theta_1 = -\theta_2$ correspond to the nodes 1 and 17 respectively. Finally, the last two boundaries, $\theta_{16} = \theta_{15}$ and $\theta_{16} = 1 - \theta_{15}$ correspond to the nodes 15 and 16 respectively. On any of the 17 walls there is an $SU(2)$ symmetry enhancement. Moreover, on the intersection of these hyperplanes we can get the group given by taking the dots in the Dynkin diagram corresponding to the intersecting hyperplanes, as discussed before.

Having described explicitly the cross section of the chimney, we are only left with the boundaries at the bottom when we introduce the radius direction. These two spherical walls correspond to small radius enhancement of gauge group by an extra $SU(2)$, and is already well known in the context of heterotic strings. Consider now, R^{17} , where the new coordinate is nothing but R_h . The chimney is bounded from below by the following two S^{16} 's,

$$R_h^2 + \sum_{i=1}^{16} \theta_i^2 = 2 \quad R_h^2 + \sum_{i=1}^{16} \left(\frac{1}{2} - \theta_i \right)^2 = 2 \quad (4.3)$$

In terms of the Dynkin diagram of Figure 1, each of these boundaries correspond to the nodes 18 and 19 respectively.

Now we are ready to give the complete parametrization of the fundamental domain of the full moduli space. In the coordinates of R^{17} defined by $(\theta_1, \dots, \theta_{16}, R_h)$, we have the following region,

$$\hat{\mathcal{M}} = \left\{ \begin{array}{l} -\theta_2 \leq \theta_1 \leq \theta_2 \\ 0 \leq \theta_i \leq \frac{1}{2}, \quad \theta_i \leq \theta_{i+1} \quad i = 2 \dots 15 \\ \theta_{15} \leq \theta_{16} \leq 1 - \theta_{15} \\ R_h^2 + \sum_{i=1}^{16} \theta_i^2 \geq 2 \\ R_h^2 + \sum_{i=1}^{16} (\frac{1}{2} - \theta_i)^2 \geq 2 \end{array} \right. \quad (4.4)$$

(the Z_2 outer automorphism noted before acts on moduli space by taking all $\theta_i \rightarrow (\frac{1}{2} - \theta_i)$)

From this explicit description and regions of enhanced gauge symmetry we can now see exactly at which points we get which enhanced gauge symmetries.

Incidentally, in terms of the coordinates we have introduced for the hyperbolic moduli space, its constant negative curvature metric is given by

$$(ds)^2 = \frac{1}{R_h^2} \left(dR_h^2 + \sum_i d\theta_i^2 \right)$$

There is another choice of the moduli space one can make (by an $SO(17, 1; \mathbf{Z})$ transformation) which is more adaptable to the compactification of the $E_8 \times E_8$ heterotic string. In this case we again have 19 boundaries, but the straight walls of the chimney correspond to the 18 nodes of the extended Dynkin diagram of the two E_8 's. The last node corresponds to a sphere corresponding to the bottom of the chimney. The direction of increasing the ninth radius for the $E_8 \times E_8$ theory corresponds to going along the linear direction of the chimney. Again the cross section of the chimney for large R corresponds to moduli of flat $E_8 \times E_8$ connection on the circle of fixed radius.

In Figure 3 we see how the Dynkin diagram of $\Gamma^{17,1}$ can be given basis encoding the $E_8 \times E_8$ structure. The nodes $1 \dots 8$ form a Dynkin diagram of E_8 and so do the nodes $1' \dots 8'$. Adding the nodes A and A' to each of the E_8 's makes them affine \hat{E}_8 . These two affine versions of E_8 give the structure of the section of the chimney. Finally, the node labelled by B represents the sphere bounding the bottom of the chimney in the 17-th direction parametrized by R_h .

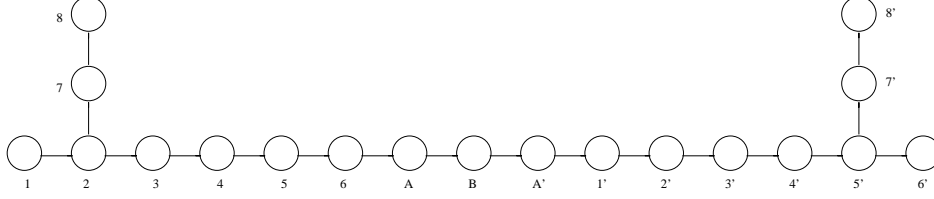


Figure 3: Generalized Dynkin diagram for $\Gamma^{17,1}$. The basis are chosen to show the embedding of the Dynkin diagram of $E_8 \times E_8$ explicitly.

5. Resolution of the Puzzles and Incompleteness of Type I'

Let us start the analysis by considering a simple example that contains all the important features of how the perturbative type I' description is incomplete and resolve the apparent contradiction of section 3.

Consider the heterotic $SO(32)$ string compactified on S^1 . If we do not turn on any Wilson lines we obtain an $SO(32)$ gauge symmetry in 9 dimensions (for sufficiently large radius). There is however another inequivalent choice of Wilson line which also yields an $SO(32)$ gauge symmetry in 9 dimensions. Consider acting by a Z_2 symmetry as we go around the circle, where the Z_2 acts as -1 on the states which are weights in the spinor of $SO(32)$ and $+1$ on the other weights. This also preserves an $SO(32)$ gauge symmetry because the root lattice is invariant under the Z_2 . From the viewpoint of type I (or type I') theory, the two choices are the same at the perturbative level, because there are no states in the perturbative type I theory transforming according to the spinor of $SO(32)$. Let us connect these two classes of theories with a continuous choice of Wilson line. In particular consider the Wilson line given by $\theta = (0^{15}, \lambda)$. For generic λ and generic radius the unbroken gauge group is $SO(30) \times U(1)^3$. The $\lambda = 0$ corresponds to turning on no Wilson line, leaving an $SO(32)$ gauge symmetry. The choice $\lambda = 1$ correspond to the Z_2 Wilson line, which acts only on the spinor degrees of freedom, again leaving an $SO(32)$ gauge symmetry. The heterotic moduli space for fixed coupling is a strip in the $(R_h - \lambda)$ plane that is unbounded on one side since R_h can be arbitrarily large but bounded on the other by the condition that $R_h^2 \geq R_{hc}^2 = 2(1 - \lambda^2/2)$. The width of the strip is given by the condition that $0 \leq \lambda \leq 1$ as discussed before. This moduli space is shown in Figure 4. This is simply a 2-dimensional slice of the chimney moduli space we discussed in the previous section.

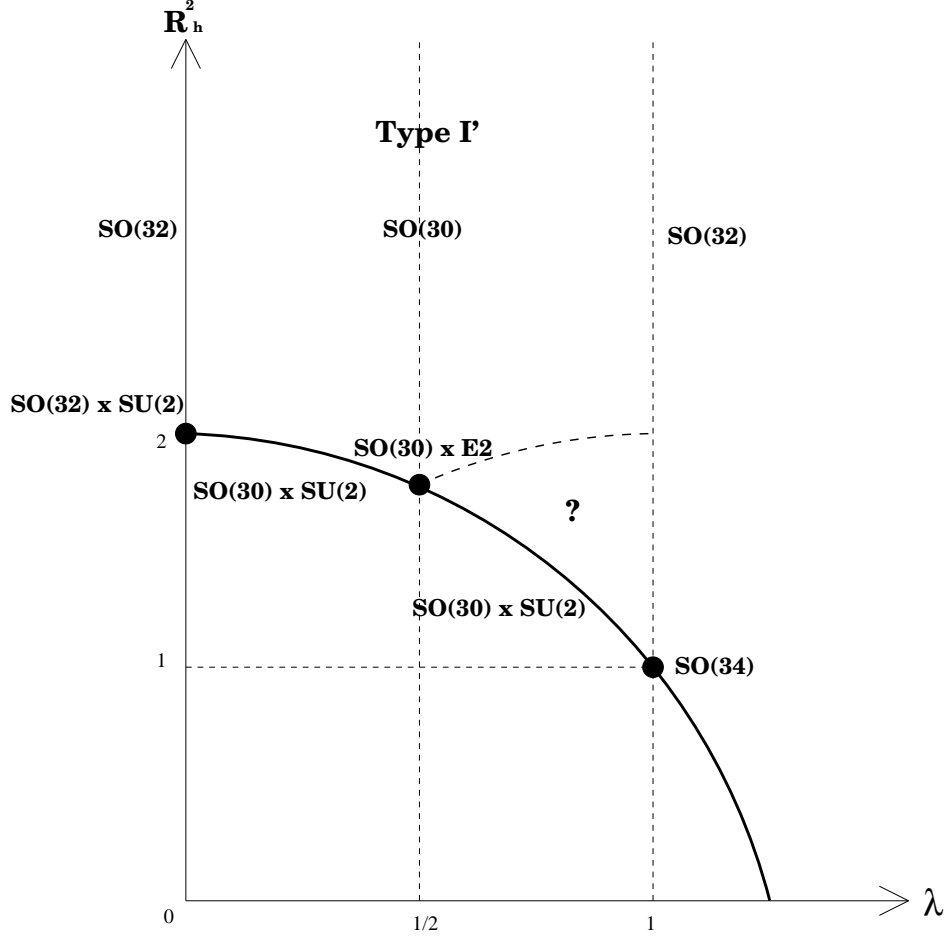


Figure 4: 2-dimensional slice of the chimney moduli space parametrized by R_h and $\theta_I = (0^{15}, \lambda)$. The solid curved line is the critical radius for a given λ . The dashed curved line is the Type I' boundary that has no extra massless particles.

Starting at a generic point – i.e., not in the boundary – we can make the radius smaller until we hit the $R_h^2 = 2(1 - \lambda^2/2)$ boundary at which an $SU(2)$ gauge symmetry will appear in addition to the $SO(30)$ we had. Starting again from the same generic point but moving in λ we can hit either the $\lambda = 0$ or $\lambda = 1$ boundaries, at any of them we get an $SO(32)$. Now if we go down in the radius direction for $\lambda = 0$ we will hit the $R_h^2 = 2$ boundary getting an $SO(32) \times SU(2)$ gauge group while in the case $\lambda = 1$ the critical radius is at $R_h^2 = 1$ with an $SO(34)$ enhancement. This follows from our discussion of the global aspect of the moduli space and points of gauge symmetry enhancement (the circle corresponds to the 18-th node on the extended Dynkin diagram, and the 16-th node in this case maps to line $\lambda = 1$ which together with other nodes coming from $SO(30)$ will form $SO(34)$).

Let us try to follow the previous paths but from the Type I' view point. Turning on λ corresponds to moving one of the 16 D8 branes away from one orientifold. With the conventions we have used this corresponds to the position x of the D8 brane changing from 0 to 4π as we vary λ from 0 to 1. At $\lambda = \frac{1}{2}$ the D8 brane is on the opposite orientifold plane. Continuing to increase λ beyond this value from the viewpoint of the Type I' theory does not change the perturbative theory at all, since it is equivalent to taking the image D8 brane back to the orientifold we started with.

However now let us repeat the same process but tune the Type I' coupling so that $1/g = 0$ at the other orientifold. If $\lambda = 0$ this corresponds to the gauge symmetry enhancement $SO(32) \times SU(2)$. However now consider $1/g = 0$ at the other orientifold but at $\lambda = 1$. What gauge symmetry do we expect in this case? To answer this we have to know what is the map of the type I' parameters and heterotic parameters in this regime. This is actually easy: Turning on or not turning on the Z_2 Wilson line acting only on the spinors does not affect the map between the radius of the circle viewed in the heterotic string R_h and the coupling parameters of Type I or its perturbative dual Type I'. Thus again at $R_h^2 = 2$ we find that $1/g = 0$ at the other orientifold. But for $\lambda = 1$ and $R_h^2 = 2$ there is no gauge symmetry enhancement expected on the heterotic side! In fact in the whole (λ, R_h) plane the map between heterotic and type I' variables, can be obtained by restricting attention to the $\lambda < 1/2$ because of the perturbative $\lambda \rightarrow (1 - \lambda)$ symmetry of type I' and since the value of the coupling constant in the type I' theory are fixed by supergravity solutions and that also reflects only perturbative aspects of type I'. Thus the region of validity of type I' perturbation is in the interior of

$$R_h^2 \geq 2 \left(1 - \frac{\lambda^2}{2}\right) \quad \text{and} \quad R_h^2 \geq 2 \left(1 - \frac{(1 - \lambda)^2}{2}\right)$$

Thus in particular the region in the vicinity of where $SO(34)$ gauge symmetry enhancement is to take place is not reachable by type I' perturbation theory!

Now we come to the puzzle raised in [21]: The puzzle they raised was that since all regions of moduli space are reachable without passing through points where extra massless particles appear, then perturbation has no reason to break down. However, we are proposing here that the Type I' perturbation is breaking down without the appearance of extra massless particles, namely all the points where $\lambda > \frac{1}{2}$ and $R_h^2 = 2(1 - \frac{(1-\lambda)^2}{2})$. We now argue this is not very surprising and there are already well known examples of this in quantum field theories. Consider 2d supersymmetric sigma model on the blow up

of an A_1 singularity of $K3$. This is parametrized in the sigma model by a Kahler class, the size r of \mathbf{P}^1 and a B-field on \mathbf{P}^1 , which is a θ angle. The perturbative description of sigma model corresponds to defining $g^2 = 1/r$. In particular if r is large there is a well defined perturbative description of the theory. Now go to the limit where $r \rightarrow 0$. In this limit the perturbation breaks down, and one expects to end up with a singular theory with arbitrary light mass states. This expectation is borne out as long as $\theta = 0$. However if for example $\theta = \pi$ this turns out not to be true. In fact as was shown by Aspinwall [31] in this case one obtains the orbifold conformal theory on R^4/Z_2 , which is perfectly well behaved. Mathematically what is going on is roughly that in the correlation function we have objects which behave as

$$1/(1-x)$$

where $x = \exp(-r + i\theta)$. The perturbative regime corresponds to $x \sim 0$. The radius of convergence of perturbation expansion is $|x| < 1$. However if we put $x = -1$, which corresponds to $\theta = \pi$ there is no singularity in the correlation, but nevertheless the perturbative description breaks down. This is parallel to what we believe happens to perturbative description of type I'.

Let us now give further evidence for this, related to D4 brane probe in the context of the example we just discussed. Consider the point where $\lambda = \frac{1}{2}$ and take $1/g = 0$ on the other orientifold. This corresponds to having an $SU(2)$ symmetry at the other orientifold point. Now put the D4 brane probe also at the orientifold. Then on the D4 brane probe lives a superconformal theory, which is equivalent to M-theory in a local CY 3-fold geometry where we have a P^2 blown up at 2 points shrunk to zero size. This is called the E_2 conformal theory, and flow upon deformation to an $SU(2)$ with one massless fundamental flavor. The mass of the fundamental field corresponds roughly to $m = \frac{1}{2} - \lambda$. It was shown that for $m > 0$ and $m < 0$ give rise to two inequivalent conformal theories, corresponding to an $SU(2)$ theory on the probe, with or without a discrete Z_2 valued θ angle in the gauge theory. The theory with the Z_2 valued θ angle turned on is expected to have *no global symmetry* even though the D4 probe is placed at the orientifold with the value of the coupling $1/g = 0$. The absence of extra global symmetries in this case, means in particular that the target space has no extra gauge symmetries, *even with vanishing* $1/g = 0$ at the orientifold. This we identify with the line emanating from $\lambda > \frac{1}{2}$ and with $R_h^2 = 2(1 - \frac{(1-\lambda)^2}{2})$, which has no extra gauge symmetry. We can in fact do better. Namely we can map the moduli space expected from the transitions of P^2 blown up at 2 points,

which is discussed in detail in [17] (shown in Fig. 5) with that given by the parameters of the heterotic string near $\lambda = \frac{1}{2}$ and $R_h^2 = \frac{7}{4}$.

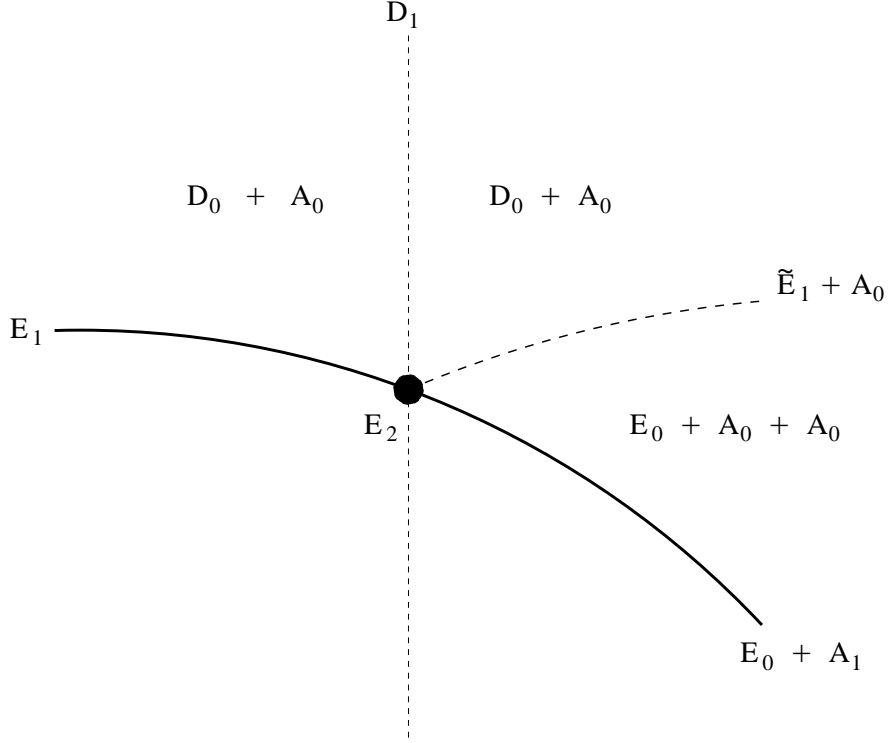


Figure 5: *Moduli space around the E_2 point for vanishing Del Pezzo surfaces or 5-dimensional field theories at non-trivial superconformal fixed points.*

Here the A, D, E 's in the above figure represent global symmetries expected from the del Pezzo description where A_0, D_1, \tilde{E}_1 correspond to a $U(1)$ symmetry, E_1, A_1 corresponds to $SU(2)$ and E_0 corresponds to no global symmetry.

The above figure should also represent (part of) the moduli of Type I' theory if the conformal theory description found from del Pezzos match parameters seen by the D4 brane probe. Moreover the global symmetries of the conformal theory predicted from the del Pezzos should correspond to gauge symmetries of the bulk type I' theory, inherited by the D4 brane probe. Indeed, we see an isomorphism between the above figure and the moduli of type I' given in figure 4 near $R_h^2 = \frac{7}{4}$ and $\lambda = \frac{1}{2}$, suggesting a type I'-like description may be valid. In fact the extra gauge symmetries anticipated from the heterotic string moduli exactly matches the global symmetries anticipated from the del Pezzo description of the conformal theory. In particular the dashed line should correspond to *no enhanced gauge symmetry* as \tilde{E}_1 has only a $U(1)$ global symmetry. The solid line

represents on the heterotic side a region with an extra $SU(2)$ symmetry and this also matches the del Pezzo prediction, as on either side of the E_2 point we have an $SU(2)$ global symmetry. However, to the left of E_2 the global symmetry is part of the symmetry seen by the conformal theory, whereas on the right side the global symmetry is a symmetry of the massive particles. Moreover in the region below the dashed line and above the solid line there is no enhanced gauge symmetry in agreement with the fact that the global symmetry there is expected to be $U(1) \times U(1)$.

If one tries to force a complete type I'-like description in all regions of the above moduli space, one sees that in bulk language, the A_0 's should correspond to D8-branes, but there is a region between the dashed curve and the solid line with $E_0 + A_0 + A_0$ where it seems that there are two branes instead of one as we started with! This is precisely in the region where we have argued Type I' perturbation does not apply. There was a picture suggested by Morrison and Seiberg [17], which tries to extend the type I' description, beyond the regime of its validity by forcing a type I'-like description. This involved the assumption that we can extract one extra brane out of the orientifold at infinite coupling. This should be only possible when the orientifold with the infinite coupling is correlated with the other choice of the discrete Wilson line, so that it does not give rise to an enhanced gauge symmetry. For instance going back to the region which was missing in type I' theory they would assign a 17th D8-brane, whose position is related to the R_h . Let us recall that the horizontal direction is controlled by the value of the Wilson line and the vertical direction by the heterotic radius. Below the line with $\tilde{E}_1 + A_0$ the value of the Type I' coupling at the orientifold is frozen to be $1/g = 0$, therefore the radius should be controlling the position of the “new brane” that is pulled out from the orientifold. More precisely, the radius is controlling the relative position between the “new brane” and the old brane. For any Wilson line $\frac{1}{2} < \lambda < 1$ we get that at the critical radius (solid line in Figure 4) the relative position is zero and the two A_0 's form an A_1 in the E_0 theory on the D4-brane probe. Something especial happens at $\lambda = 1$ since the two branes reach the other orientifold with the 15 branes giving altogether 17 branes at the orientifold. This is the $SO(34)$ point.

Having described the suggested picture for explaining the $SO(34)$ point one could also ask about other possible enhanced gauge symmetry points, for example $SU(18)$ which according to our discussion is allowed. In this case if we pull one extra brane from each orientifold, this can be achieved by 18 coincident branes in the middle of the interval. This was in fact suggested to be possible in [17].

The fact that on the dashed line in figure 5 the type I' breaks down without the appearance of massless particles is somewhat novel. It is natural to ask if anything special happens there as viewed from the heterotic side. As we have argued no extra massless states appear. However, the conformal theory seen by the D4 brane is interpreted on the heterotic side as the theory seen by a single 5 brane wrapped around S^1 . Thus the heterotic theory also “knows” something special is happening there: There appears a non-trivial conformal theory on a single wrapped 5 brane. This is quite a novel effect.

Viewed from the heterotic moduli we can describe exactly which piece of the moduli space the Type I' perturbation misses. In our global description of moduli space the bottom of the chimney was described by two spheres. All we have to do is to reflect the two sphere by replacing $\theta_1 \rightarrow -\theta_1$ in the second sphere of (4.3) and $\theta_{16} \rightarrow (1 - \theta_{16})$ in the first sphere. This gives us altogether 4 spheres. The Type I' perturbation is exactly the top part of the chimney bounded by the first sphere it encounters as one decreases R_h .

Explicitly, the Type I' moduli space will be the chimney bounded from below by the following spheres,

$$\text{Physical Boundaries :} \quad R_h^2 + \sum_{i=1}^{16} \theta_i^2 = 2 \quad R_h^2 + \sum_{i=1}^{16} \left(\frac{1}{2} - \theta_i\right)^2 = 2 \quad (5.1)$$

$$\text{Pert. Breakdown :} \quad R_h^2 + (1 - \theta_{16})^2 + \sum_{i=2}^{16} \theta_i^2 = 2 \quad R_h^2 + \sum_{i=1}^{15} \left(\frac{1}{2} - \theta_i\right)^2 + \left(\frac{1}{2} + \theta_1\right)^2 = 2 \quad (5.2)$$

It is interesting to see how the possibility of having one or two extra branes fits with filling the 3 missing regions of the moduli space. At a qualitative level, we have already explained how this would arise. In particular let us consider the region where we have 2 extra branes. Let us denote by $x_0, x_1, \dots, x_{16}, x_{17}$ the positions of the 18 branes, and let us say that the first 17 are independent. The two boundaries on the bottom of the “chimney” describing the moduli space are now represented by $x_0 = x_1$ and $x_{16} = x_{17}$, where the mechanism for the generation of $SU(2)$ enhanced gauge symmetry is the same as in the usual perturbative type I'. This should fill the region in moduli space given by

$$-\theta_2 < \theta_1 < 0, \quad 1/2 < \theta_{16} < 1 - \theta_{15}$$

$$0 < \theta_2 < \theta_3 < \dots < \theta_{15} < 1/2$$

$$R_h^2 + \sum_{i=1}^{16} \theta_i^2 > 2 \quad R_h^2 + \sum_{i=1}^{16} \left(\frac{1}{2} - \theta_i\right)^2 > 2$$

Pert. Breakdown :
$$R_h^2 + (1 - \theta_{16})^2 + \sum_{i=2}^{16} \theta_i^2 < 2 \quad R_h^2 + \sum_{i=1}^{15} \left(\frac{1}{2} - \theta_i\right)^2 + \left(\frac{1}{2} + \theta_1\right)^2 < 2$$

Note that there are 19 boundaries in this region which match with the nineteen boundaries for of $0 < x_0 < x_1 \dots < x_{17} < 2\pi$. Similar statement can be made about the other regions where only one extra brane appears.

Now we can try to generalize (2.5) from the Type I' analysis of section 2 in order to describe this situation in a more quantitative form. For instance, in the case where we get two extra branes and the inverse coupling is frozen to zero at both orientifolds, the most natural thing to write is,

$$z(x) = \frac{3}{\sqrt{2}} \left(\frac{1}{2} \sum_{I=0}^{17} x_I - \frac{1}{2} \sum_{I=0}^{17} |x - x_I| \right) \quad (5.3)$$

This reproduces the D4-brane expectations for the coupling constant when it is expressed in terms of the proper distances as in (2.8)⁷

Even though this completion of type I' is compelling and matches various aspects of heterotic gauge theory enhancement one expects, it is clearly beyond the regime of the type I' perturbation theory. For example on the D4 brane probe after we pull the extra brane off the orientifold we do not expect to have an $SU(2)$ gauge symmetry. Also we have no good explanation of these extra branes, and apart from matching with expected behavior from the heterotic theory, it seems ad hoc. We will try to give a unified description of all regimes of parameters of type I' based on geometry of real elliptic $K3$ in the remaining sections.

⁷ We can try to go even further and try to match the parameter of the moduli of type I' with those of heterotic strings. It is natural in the region we just discussed, to introduce two new θ 's, namely θ_0 and θ_{17} . We define them by

$$\theta_0 = -\frac{1}{2} \left[R_h^2 + \left(\frac{1}{2} + \theta_1\right)^2 + \sum_{i=2}^{16} \left(\frac{1}{2} - \theta_i\right)^2 - 2 \right]$$

$$\theta_{17} = \frac{1}{2} \left[R_h^2 + (1 - \theta_{16})^2 + \sum_{i=1}^{15} \theta_i^2 - 1 \right]$$

The choice of these values are motivated by the condition that when $\theta_0 = 0$ and $\theta_{17} = \frac{1}{2}$ should correspond to the boundaries (5.2) and $\theta_0 = -\theta_1$ and $\theta_{17} = (1 - \theta_{16})$ should correspond to (5.1). Then using the map between brane positions and the Wilson loop expectation values given by (2.11) we can relate the 18 x_i 's brane positions with the 18 θ 's, which are in turn captured by the 17 moduli parameters of heterotic strings.

6. Real Elliptic $K3$ as a limit of F-Theory

Type IIA on $K3$ is dual to heterotic string on T^4 . This duality can be pushed up one dimension by considering the strong coupling limit of type IIA, where we obtain M-theory on $K3$ being dual to heterotic on T^3 . If we view $K3$ as an elliptic manifold over \mathbf{P}^1 and consider the limit where the elliptic fiber goes to zero size, we should obtain a description involving type IIB on \mathbf{P}^1 with 24 various (p, q) type 7-branes. This is the F-theory description. This can also be viewed as type IIB compactified on T^2 modded out by a Z_2 with an orientifold action [24]. If the branes are not equally distributed among the orientifold planes the theory become non-perturbative in the type IIB language and has a description which is captured by the geometry of the elliptic $K3$.

The question is whether this geometric description can be continued one more step to provide a strong coupling description of heterotic strings in 9 dimensions. As we have found in the previous sections, type I' description is inadequate, and it would be interesting to see if geometry sheds any light on some of the questions raised in that context.

What we should do is to ask how the radius of the 8-th direction is encoded in the geometry of elliptic $K3$ and use this to obtain the limiting geometry as the radius in the 8-th direction goes to infinity. Before doing this, it turns out to be convenient first to review the situation in going from 7 dimension to 8 dimension; i.e. in going from M-theory on $K3$ to F-theory on elliptic $K3$.

Consider heterotic strings on T^3 . Its moduli space is captured, in addition to the string coupling, by the moduli of the $\Gamma^{19,3}$ lattice. Note that this is directly related to the geometry of $K3$, namely, the lattice is identified with the H_2 lattice on $K3$ and the choice of the metric on $K3$ determines the splitting to left and right part of the lattice by the action of $*$ -duality induced by the metric. The overall radius of $K3$ does not enter the duality operation and is related to the inverse of heterotic string coupling constant.

Now if we are interested in going to 8 dimensions, we consider the limit where T^3 is given by $T^2 \times S^1$ with a large radius for S^1 . Let us consider the metric (including the anti-symmetric B-field) on T^3 in a block diagonal form, respecting this decomposition. We can also turn on Wilson lines on S^1 , but clearly in the limit of going to 8 dimensions, they are irrelevant. So let us consider turning them off around the S^1 . The moduli space of this subset of 7 dimensional compactifications is given by the moduli of polarizations on $\Gamma^{18,2} + \Gamma^{1,1}$ respecting this decomposition. The moduli of $\Gamma^{18,2}$ is parametrized by 18 complex parameters, and that of $\Gamma^{1,1}$ by one real parameter. This real parameter is in

fact identified in the usual way with the radius of the seventh circle. Thus in going to 8 dimensions the geometry of $\Gamma^{18,2}$ remains intact. Now we ask how this is realized in the geometry of $K3$. The most natural way to say this is as follows: Consider the inversion map on the 7-th circle in the heterotic side $x^7 \rightarrow -x^7$. This is a symmetry of heterotic strings if there is no Wilson line on the circle as well as if the metric is block diagonal on $T^2 \times S^1$. In particular it acts on the $\Gamma^{19,3}$ lattice. Let us combine this, with an overall Z_2 inversion of the full $\Gamma^{19,3}$ lattice. We thus see that we have a Z_2 symmetry which acts as

$$\Gamma^{19,3} \rightarrow \Gamma_{(-)}^{18,2} + \Gamma_{(+)}^{1,1} \quad (6.1)$$

On the $K3$ side this symmetry should be realized as a Z_2 symmetry on the geometry acting on the 2-cycles of $K3$ exactly according to this decomposition. Moreover one should choose a metric on $K3$ respecting this Z_2 symmetry. In the context of F-theory, this Z_2 is realized by

$$y \rightarrow -y, \quad x \rightarrow x, \quad z \rightarrow z \quad (6.2)$$

which is a symmetry of elliptic $K3$ given by

$$y^2 = x^3 + f(z)x + g(z)$$

with f and g being polynomials of degree 8 and 12 respectively. The elements of H_2 invariant under the Z_2 correspond to the class of the elliptic fiber E and the base $B = P^1$. They have an intersection given by

$$E^2 = 0, \quad B^2 = -2, \quad E \cdot B = 1$$

which defines the $\Gamma^{1,1}$ lattice where if we define

$$e_1 = E + B, \quad e_2 = E$$

we get the standard description of inner product for $\Gamma^{1,1}$. Note that under the Z_2 defined in (6.2) the classes E and B are invariant. That the base class is invariant is obvious, as that is parametrized by z . That E is invariant follows from the fact that the $(1,1)$ form corresponding to it, has even number of y and \bar{y} 's (recall the $(1,1)$ form is given by $|dx/y|^2$). It is also possible to show that the other 20 classes in H_2 are mapped to minus themselves. This follows by viewing them roughly speaking as products of 1-cycle in the base and 1-cycle in the fiber. Note in this context that the radius of the heterotic

string is related to the sizes of E and B through the map given above. Namely, if we identify e_1 with the winding vector $(P_L, P_R) = (-R, R)$ and e_2 with the momentum vector $(P_L, P_R) = (1/R, 1/R)$, and use the BPS formula for P_R which is proportional to the integral of the kahler form over the corresponding class we learn that

$$\frac{\int_{E+B} k}{\int_E k} = R^2$$

which leads to

$$k(B)/k(E) = R^2 - 1 \tag{6.3}$$

In particular the limit $R \rightarrow \infty$ for a fixed volume of $K3$, corresponds to taking $k(B) \sim R$ and $k(E) \sim 1/R$, which is the usual statement that in the limit of zero size elliptic fiber, compared to the base, we obtain a geometry which captures the moduli space of heterotic strings on T^2 .

Now we repeat this same idea, but in taking the limit from F-theory on elliptic $K3$ and follow the moduli of $K3$ in the direction of decompactifying a circle of heterotic string. Again if we turn off the Wilson lines on the circle we are decompactifying, this means we will have additional Z_2 symmetry in the theory, which acts exactly as the one we discussed above in the context of going from 7 to 8 dimensions, namely the action (6.1) on the H_2 lattice. Taking into account both Z_2 's, we can thus decompose the lattice as

$$\Gamma^{19,3} \rightarrow \Gamma_{--}^{17,1} + \Gamma_{+,-}^{1,1} + \Gamma_{-,+}^{1,1}$$

Note in particular that the new Z_2 we want should act as inversion of the $\Gamma^{1,1}$ lattice corresponding to the original E and B of the F-theory.

The main question to ask now is which subclass of $K3$'s is relevant for which there is such a symmetry? The main hint comes as follows: In going from 10 to 8 dimensions, the Wilson lines of the heterotic string around the 2-circles correspond to complex moduli:

$$u^i = A_9^i + iA_8^i$$

with real A_8 and A_9 . The complex parameters u^i should be identified with (some of) the complex coefficients defining f and g in F-theory on $K3$. Turning off the Wilson lines in the 8-th direction, would make the parameters u^i real. We are thus led to look for elliptic $K3$'s with real coefficient. The Z_2 symmetry, which flip the 8-th circle, will act on $A_8 \rightarrow -A_8$, and so will take $u^i \rightarrow u^{i*}$. Thus the Z_2 symmetry we would like to define

on $K3$ should be a real involution symmetry, which would require the coefficients u^i to be real. Thus we look for elliptic $K3$'s which are real, i.e. which are of the form

$$y^2 = x^3 + f_8(z)x + g_{12}(z)$$

where f and g are real polynomials respectively of degree 8 and 12 in z , and the Z_2 symmetry we are after acts on $K3$ as

$$y \rightarrow y^* \quad x \rightarrow x^* \quad z \rightarrow z^*$$

Furthermore we would like to make sure that the Z_2 acts on the H_2 homology according (6.1). That it acts on E and B of F-theory in the right way, is easy to check. However, we also need to check that it acts correctly on the rest of the homology elements of $K3$. It turns out, as we will now discuss, this puts restrictions on the coefficients of f_8 and g_{12} .

All real involutions on $K3$ have been classified by Nikulin [32] with the following conclusion: Consider the fixed locus of the Z_2 involution in $K3$. Let us call this the real $K3_R$. In other words

$$K3_R \subset K3 \quad (K3_R)^* = K3_R$$

It is clear by dimension count that $K3_R$ is a 2-dimensional real subspace of $K3$. It has been shown by Nikulin, that $K3_R$ is in general not a connected surface. In particular, depending on the Z_2 real involution, it consists of k spheres, together with 1 genus g surface. Moreover not all k and g can appear. The allowed ones are shown in the figure below:

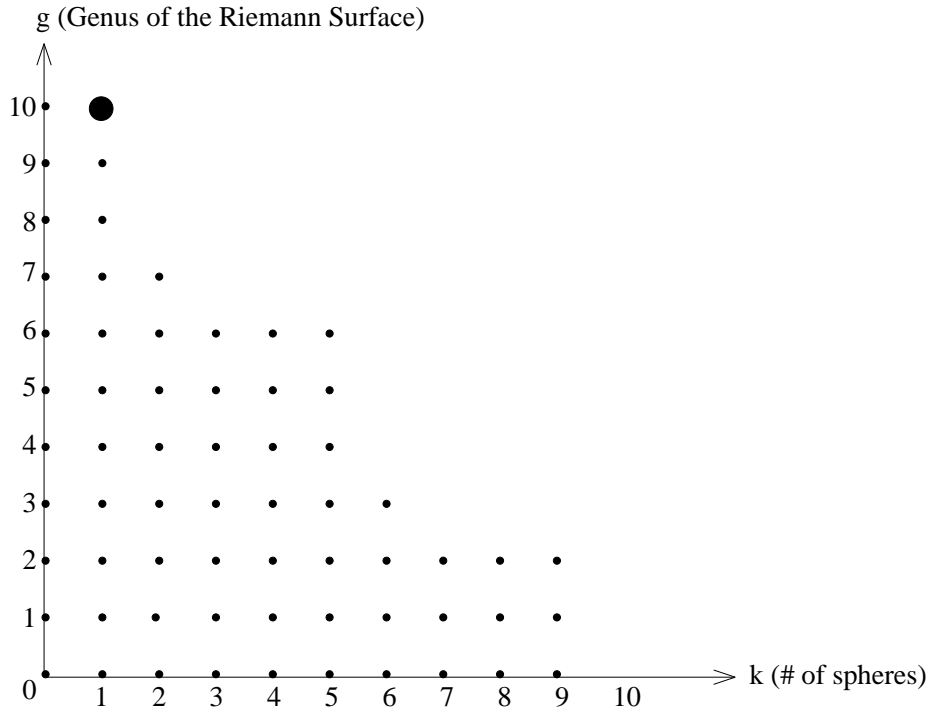


Figure 6: *Classification of Real K3 surfaces according to the genus (g) of the Riemann Surface and the number (k) of spheres. Small dots represent the allowed values for (k, g) and the big dot is the one corresponding to the Real K3 related to the heterotic string in 9 dimensions.*

The k and the g one gets is determined by the Z_2 action on the H_2 . For the Z_2 action we are interested, given by (6.1) we find $k = 1$ and $g = 10$. In other words we have

$$K3_R = S^2 + \Sigma_{10} \subset K3$$

where Σ_{10} denotes a genus 10 Riemann surface.⁸ Nikulin's classification also applies to holomorphic involution which takes the holomorphic 2-forms to minus itself; in fact by an $SO(3)$ rotation in the choice of complex structure, the two are equivalent. In other words, even the involution that we used in the context of F-theory, could be viewed as a real involution for a particular choice of complex structure on $K3$. In that case, we can also check that the structure of $K3_R$ i.e. the subspace fixed by the Z_2 involution $y \rightarrow -y$ is as we have: the fixed point of $y \rightarrow -y$ corresponds, for each point on the z -plane to four points on the torus, the three roots of the cubic, plus the point at infinity, corresponding to $x = \infty$. As we vary z we get a surface. The point $x = \infty$ does not mix with the others, and gives a copy of the base \mathbf{P}^1 . The other roots exchange and give a three fold cover of the base, which turns out to have genus 10. This is easy to see. The Riemann surface is given by the equation

$$x^3 + f(z)x + g(z) = 0$$

where f and g are polynomials of degree 8 and 12 respectively. Its Euler characteristic χ can be computed by removing the 24 points on z sphere where roots of the cubic coincide, computing its Euler characteristic (which is 3 times that of the sphere without 24 points)

⁸ There is a simple index theory argument which shows why, if we have only one sphere, i.e. if $k = 1$, the genus of the extra component $g = 10$. To see this let h denote the Z_2 anti-holomorphic automorphism. Then h acts on the cohomology of $K3$ and by Lefschetz fixed point theorem we know that its trace on the cohomology (weighted by $(-1)^{degree}$) should be the Euler characteristic of the fixed point set. This gives, since we know the action of h on the mid-dimension cohomology (as well as the fact that h acts trivially on the H^0 and H^4) that

$$2 + (2 - 2g) = 4 - 20 = -16$$

which implies that $g = 10$.

and then adding two points for each removed point (because two of the x 's meet at each of the 24 points). We thus have

$$\chi = 3(2 - 24) + 2(24) = -18 = 2 - 2g \quad \rightarrow g = 10$$

Here we want to give a concrete description of the real $K3$, which also explains why we can have multiple components. To describe $K3_R$ we consider real solutions (i.e. real (x, y, z)) of the real equation $y^2 = x^3 + f(z)x + g(z)$. We can view the real z (including infinity) as the equator in the complex z -sphere base of F-theory, and real x, y subject to the above equation as real circle or circles in the elliptic fiber of F-theory. Note that there can be one or two real circles for each real value of z depending on the sign of the discriminant of this equation $\Delta = 4f^3 + 27g^2$. If Δ is positive, the solution is homeomorphic to a single circle (including the point ∞ to the (x, y) plane). However, if Δ is negative, the solution is homeomorphic to two disconnected circles.

The $K3_R$ can be viewed, therefore, as one or two circles fibered over the equator given by real z . Note however, that the number of circles can change. This happens if as we change z the discriminant $\Delta = 0$. Let us assume that Δ has a single zero at $z = z_0$. This implies that Δ should change sign and therefore the real fiber over the z in a neighborhood of $z = z_0$ will have to interpolate between a fiber with two components to a fiber with only one or vice versa depending on the way Δ changes. It is clear that $f(z_0) < 0$ and $g(z_0) \neq 0$. This is true because if $g(z_0)$ and $f(z_0)$ were zero then Δ would have at least a zero of order two. This makes clear that there are two possibilities characterized by the sign of g at $z = z_0$.

For g positive the transition takes place when the two circles approach each other, join at one point and then open up to give a single circle. For g negative one of the circles shrinks to a point and then disappear. All this is shown in Figure 7.

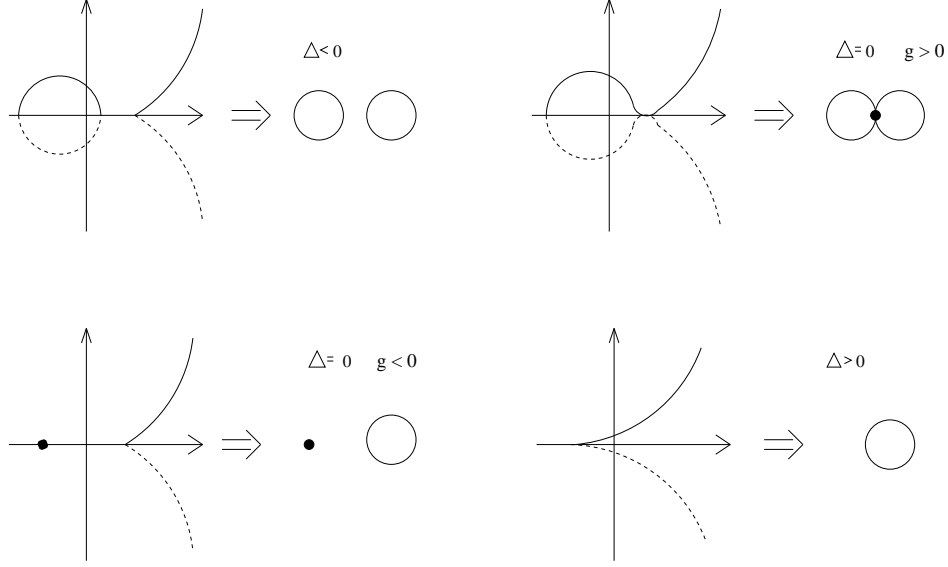


Figure 7: Classification of the possible Real fibers according to the sign of Δ for $\Delta \neq 0$ and to the sign of g for $\Delta = 0$.

It is important to notice that the circle containing the point ∞ in the (x, y) plane is always present for any z . If we vary z over \mathbf{R} and add $z = \infty$ we will necessarily get at least one Riemann surface of genus ≥ 1 .

Now we are ready to describe the possible transitions involving two consecutive single zeros of Δ . There are only four possibilities if we start and end with single components, i.e., with $\Delta > 0$. Three of them are shown in Figure 8A, 8B and 8C. The fourth is just a reflection of Figure 8A. In Figure 8D we have shown a transition where we start and end with $\Delta < 0$ and the points with $\Delta = 0$ have $g < 0$ and $g > 0$ respectively from left to right. In this case it is easy to show that $f(z)$ must have two real zeros (denoted by white dots) between the two branes (denoted by black dots).

It is clear now that transitions of the B type will increase the genus of our “basic” Riemann surface and transitions of the C type will leave invariant the topology of the basic Riemann surface but will add an extra component that can only be a sphere!

Finally, the transitions of the A and D type do not change the topology of the Real $K3$ but will play an important role later on.

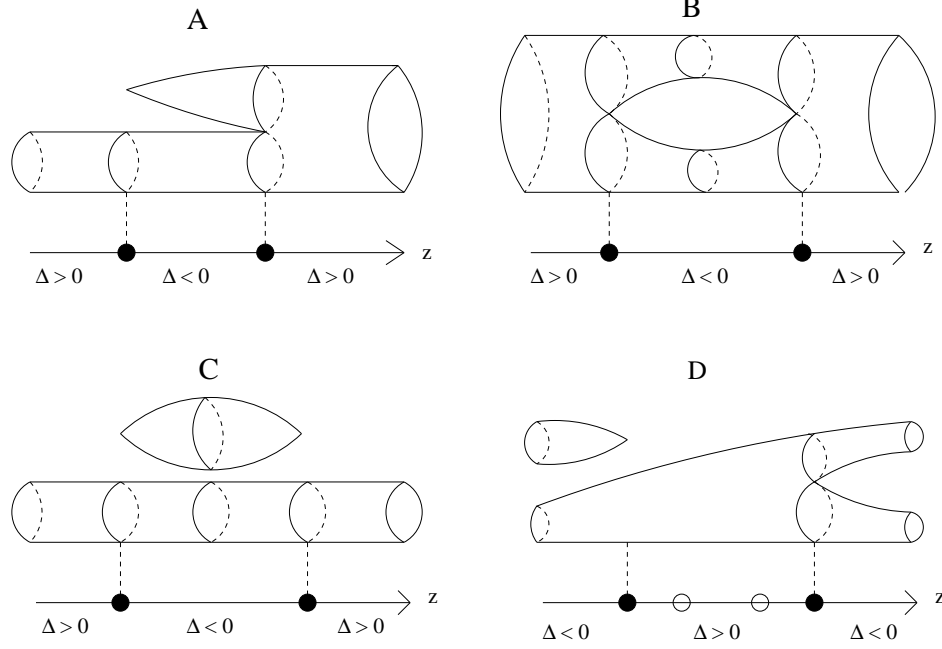


Figure 8: Some possible sections of a real $K3$ in an interval containing two single singular fibers.

7. General Aspects of Real $K3$ and the moduli space in 9 dimensions

In this section we discuss some general aspects of real $K3$ and how it relates to the moduli space in 9 dimensions. We will see explicitly how the type I' branes (and their generalization) have a natural interpretation in this language. We will divide our discussion into two parts: qualitative and quantitative.

7.1. Qualitative analysis

We have argued in the previous section that the real $K3$ should have two components, one with genus 10 and another with genus 0. In other words as we go along the real z direction, we get the splitting and joining described in previous section, which makes up a sphere and a genus 10 Riemann surface. The simplest possibility is that shown in figure 9. Note that the Riemann surface with genus 10 has nine holes, plus one hole going around the z -equator. Also note that in the region in the z -axis where the real sphere arises, between $X1$ and $X2$ the genus 10 Riemann surface cannot have a hole. This is because over each point z we can have at most two circles of real $K3$. Out of the 24 points on the z sphere with vanishing discriminant Δ in the case shown here we have accounted for 20 of them: $X1, X2$ where the sphere is formed and from the points 1, ..., 18 where the 9 holes of the genus 10 Riemann surface are carved out. This leaves us with 4 extra branes which

must be in the bulk. Since f and g are real polynomials in z , so is Δ , which implies that all the roots come in complex conjugate pairs. Thus the 4 roots which are not real come in two complex conjugate pairs.

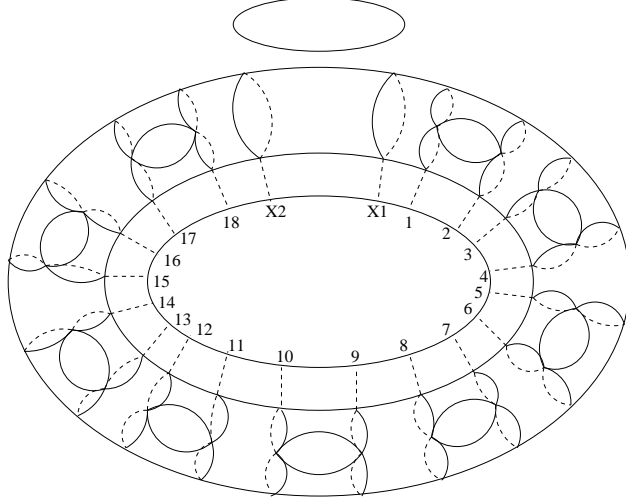


Figure 9: Real $K3$ corresponding to the case with 20 real roots.

It is natural to ask if the figure 9 is the most general possibility compatible with having a genus 10 Riemann surface and a sphere. In fact it is not. Even though one may think that bringing the branes from the bulk down to the real axis changes the topology, it is possible to preserve the condition that the genus is 10. In fact we can have configurations of two branes as shown in figure 8A which does not change the topology. We will argue later that if two pairs come down to zero it can intersect the real z axis only between the points 2 and 3 or between the points 16 and 17. So altogether we have 4 possibilities: All 4 extra branes off the real axis, one or the other pair on the real z axis (Figure 10), and both pairs on the real z axis (Figure 11). This matches very nicely the 4 possibilities predicted from the analysis of Wilson lines for $SO(32)$: As we discussed before the first brane being positive or negative relative to the orientifold position are distinct possibilities. The same being true for the last brane. Thus the four possibilities we are encountering from the real $K3$ geometry matches beautifully this aspect of the choices of inequivalent $SO(32)$ Wilson loop values.

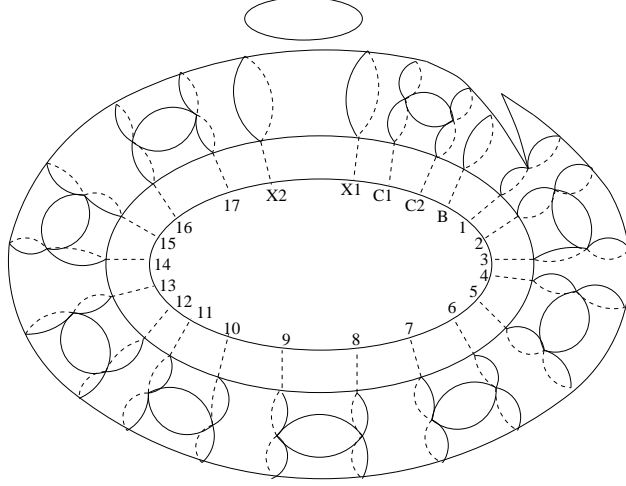


Figure 10: *Real K3 corresponding to the case with 22 real roots.*

It is helpful to give a description of the basis of two cycles of $K3$ projected onto the real $K3$, in the basis used to describe the moduli space of type I' and the modular group for the $\Gamma^{17,1}$ lattice. This is most conveniently done for the case where all four branes are on the real axis. In this case the 2-cycles of $K3$, which project onto cycles (circles) on the real $K3$ are shown in figure 11. In this form their intersection is identical with the intersection expected for the $\Gamma^{17,1}$ lattice (this is also the fastest way of understanding why the extra branes from the bulk should land at those positions on the real axis, though we give other arguments at the beginning of the quantitative section based on the $\hat{E}_9 \times \hat{E}_9$ configuration studied in [33] and its descendant). The two sphere in the real $K3$ is to be identified with the class in $\Gamma^{1,1}$ with self-intersection -2 (and is the direct analog of the base in the context of F-theory dual of heterotic string).

Let us now argue why the extra branes can intersect the real z -axis only as described in Fig. 10 and Fig. 11. Let us suppose that in Figure 10, the two branes denoted by $B1$ and 1 were located at any other position. Let us start by locating them between 7 and 8 . In this case we would have two sets of relative local fibers, one with 11 fibers and the other with 8 fibers, if we bring them together we would have an $A_{10} \oplus A_7$ singularity that clearly can not be embedded in $\Gamma^{17,1}$. In the same way it is possible to show that at any location we would get singularities that can not be realized if we want to preserve the decomposition $\Gamma^{18,2} = \Gamma^{17,1} \oplus \Gamma^{1,1}$.

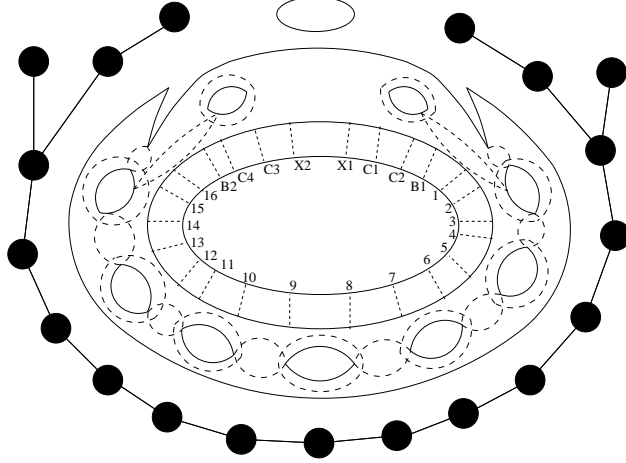


Figure 11: Real $K3$ corresponding to the case with 24 real roots. The circles correspond to the projection of the 2-cycles of $K3$ on the Real $K3$ giving the intersection structure of $\Gamma^{17,1}$

Counting Parameters

We have been considering real $K3$ in the form

$$y^2 = x^3 + f(z)x + g(z)$$

where f and g are real polynomials in z of degree 8 and 12 respectively. Thus to specify real $K3$ we have $9 + 13$ parameters going into definition of f and g minus 3 for $SL(2, R)$ symmetry which is the symmetry preserving the real structure acting on z , and an overall rescaling of the equation (the rescaling of x and y are frozen because we have chosen the coefficients of y^2 and x^3 to be one in the above equation). This gives us a total of 18 real parameters. This is exactly the right number expected based on the fact that we need to describe 16 Wilson lines and the radii of two circles, the eighth and the ninth circle, as measured say from the heterotic string side. This is of course consistent, as we discussed before with the splitting of the lattice

$$\Gamma^{18,2} \rightarrow \Gamma^{17,1} + \Gamma^{1,1}$$

where 17 parameters (16 Wilson lines and the ninth radius) go into defining the moduli of $\Gamma^{17,1}$ and the eighth radius defines the moduli of $\Gamma^{1,1}$. In fact in principle we can read off the exact point we are on the moduli, by simply measuring the volume (using the metric on $K3$) of the corresponding 2-cycles which correspond to elements in $\Gamma^{17,1}$ and those of $\Gamma^{1,1}$ (which gives the P_R components of the corresponding elements, from which we can

reconstruct the Lorentzian rotations). However, here we wish to develop some intuition in particular for the limit corresponding to going to 9 dimensions.

In going to 9 dimensions, we need to decompactify the eighth circle, which means taking the corresponding heterotic radius to infinity. As shown in equation (6.3) this means that the size of two sphere should be much bigger than the size of the elliptic class dual to it. The basic intuition we have, is in the case of F-theory, to which our situation is equivalent up to a change in complex structure. In that case the limit one takes is the elliptic fiber going to zero size. Moreover, in that limit the metric on $K3$ becomes independent of the position on the elliptic fiber (i.e. has an approximate $U(1) \times U(1)$ symmetry. Similarly here, we should first identify the analog of the elliptic fiber and then take the limit in moduli where it goes to zero size. More precisely we require that the integral

$$\int_E dz \frac{dx}{y} \rightarrow 0$$

We now need to get a better understanding of the elliptic class E dual to our sphere. It should intersect it at a point. More precisely, for every point on the real two sphere, there should exist exactly one E class, with a canonical BPS cycle chosen by minimizing the volume.

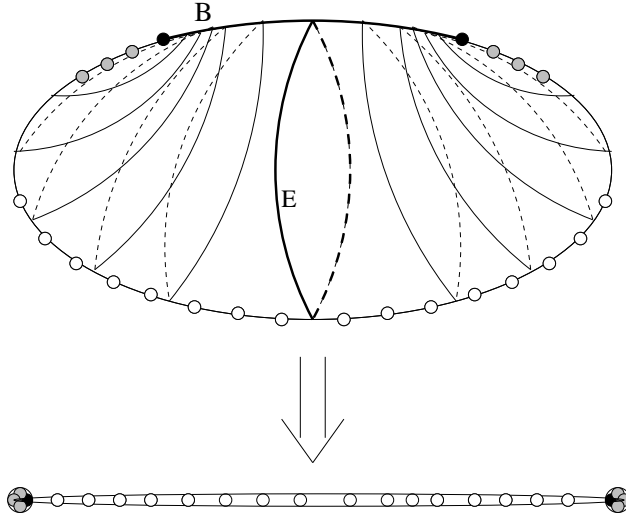


Figure 12: New elliptic fibration. The circles depicted here are the projection of the new E class representative on the z -sphere that shrink to zero. B is the projection of the new P^1 base on the old P^1 . White dots are relative local branes, black and grey dots are non local to the white branes.

The real two sphere is a circle fibered over an interval on the real z -line where at the two ends it shrinks. This circle can be identified with one of the two circles in the original elliptic fibration of F-theory. The elliptic class E dual to our real sphere, should have a cycle intersecting the cycle of the real sphere at one point, and corresponding to a cycle on the z -sphere, crossing the interval at one point transversally as shown for example in figure 12, where the image of E on the sphere is drawn as circles. The case depicted in figure 12 is when all the 24 branes are on the real axis. Note that we can also view the elliptic class as a choice of a circle in the z -plane which intersects the interval B transversally, and for which there is an invariant monodromy direction, which intersects the cycle corresponding to real sphere on the original elliptic fiber of F-theory at one point. As we change the intersection point of E with the interval B the image of E crosses some of the branes on the real z -axis. We wish to argue that precisely those that it crosses are branes of the same (p, q) type, as that of the cycle in the elliptic fiber which represents the cycle of E . This follows from the fact that as we cross the brane, represented by a class β , then the class α of E changes by

$$\alpha \rightarrow \alpha - (\alpha \cdot \beta)\beta$$

where the dot product is in the 1-cycles of the elliptic fiber. Since the infinitesimal change of the cycle should not affect the E cycle globally (in particular we could choose the same cycle near B), this implies that $\alpha \cdot \beta = 0$. In particular all the cycles that E crosses are all of the same type! This is beginning to sound like type I' as in type I' only the branes of the same type are allowed. However this also implies that the E cycle cannot cross all the branes, because they are not all local relative to one another. Indeed what we will find is that precisely for the case we have depicted in figure 12 exactly 16 of them are of the same type and the E can pass through them, and the last and first branes on either side (depicted by gray dots in the figure) will be the boundary of where the E cycle reaches. These limiting cases would correspond to when the E cycle crosses the interval B at one of its boundary points.

Now the limit of going to 9 dimensions is clear: We simply have to take the brane configurations corresponding to having zero size for *all* the cycles represented by E on the z -plane to be of zero size. This in particular means, in the case where all the 24 branes are on the real axis, that the first four and the last four approach each other (this must also necessarily shrink all the other cycles as they are all represented by the same integral). Note that now we are also left with an effectively one dimensional object, with 16 branes

on it, the boundaries of which are identified with the first and last branes (depicted by the gray dots). See Figure 12. Note that similar limits were taken in [34] but in order to get a 10 dimensional picture of the heterotic strings.

From the viewpoint of counting parameters, in this limit we see that we have naively 20 real parameters left: 16 branes in the middle, 2 positions of where each group of 4 branes has collapsed and 2 relative $SL(2, R)$ invariants from cross ratios of each of the two groups. The overall $SL(2, R)$ gets rid of 3 of them and we are left with 17 parameters which we can take to be 16 positions of the branes, and one parameter controlling the type I' coupling at one of the orientifolds given by one of the cross ratios (the other one being fixed in terms of the rest).

Here we have mainly concentrated on the case where all the 24 branes were on the real line, but we know that 2 or 4 of them could be off of it. This should correspond to bringing one brane to the orientifold and crossing it. This means taking one of the white nodes in Fig. 12 and bringing it close to the last curve of the E foliation. As that meets the first gray node, they can pair up to go to the complex plane. This corresponds to the fold disappearing off the genus 10 surface. In that case the second gray brane becomes the visible brane, i.e. becomes ‘white’, as the last foliation of E gets pushed further back (see Fig.13).

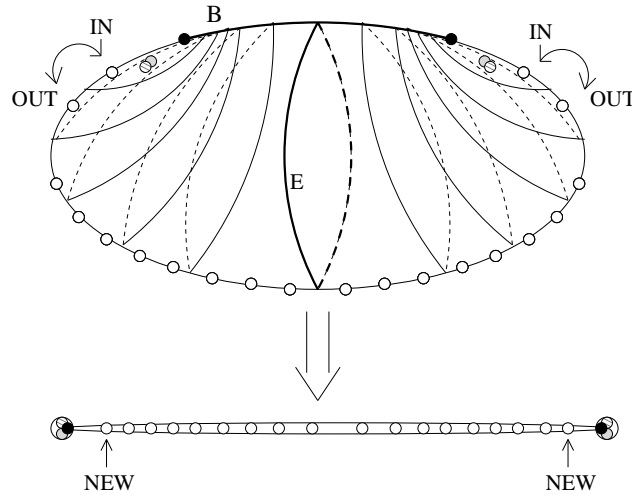


Figure 13: New elliptic fibration. The circles are the E class representative that shrink to zero. B is the projection of the new P^1 base on the old P^1 . White dots are relative local branes, black and grey are non local to the white branes. There are two branes that can be IN or OUT the minimal E cycles giving NEW white branes when they are OUT.

This we will demonstrate using monodromy arguments below. So far, even though two branes have gone to the complex plane, we are still in the regime of perturbative type I', though in the regime where $-\theta_2 < \theta_1 < 0$. Again the last curve E , which shrinks to zero size in going to 9 dimensions, has four branes in it, and thus one real parameter describes their relative moduli, which is to be identified with the coupling at the orientifold. Now as we bring the last gray brane towards the physical brane beyond some point the curve E will not include it anymore, which corresponds to pulling one extra brane out (see Fig.13). This is exactly what we were anticipating from the analysis we made of Type I' perturbation breakdown. Moreover, note that now inside the last curve of E we have 3 branes, and thus no relative moduli. This means that there is no degree of freedom associated with the orientifold, and in particular the coupling must be frozen there. We will demonstrate below, that the value is given by $1/g = 0$, completing what we expected from all the regimes of moduli of heterotic strings.

7.2. Quantitative analysis

In this part we will start by giving the monodromy analysis of the configuration of branes that we studied in the qualitative analysis. This will show that the statements we made about the monodromy along the cycle denoted by E are correct. Then we will go to the quantitative description of the 9 dimensional limit and its connection to type I' like descriptions.

Monodromy Analysis

Luckily the monodromy of various singularities relevant for us have been extensively studied in [33], whose results we will borrow (for detailed conventions we refer the reader to their paper).

In F-theory the singular fibers are associated with 7-branes of the (p, q) type (once we choose a convention of branch cuts on the \mathbf{P}^1)⁹. Let us denote the brane of (p, q) type by $X_{[p,q]}$. The monodromy around any $X_{[p,q]}$ fiber is given by

$$K_{[p,q]} = \begin{pmatrix} 1 + pq & -p^2 \\ q^2 & 1 - pq \end{pmatrix} \quad (7.1)$$

Note that when we get n branes of the same type together we get an A_{n-1} singularity. Now let us consider the case where we have all the branes on the real axis. We identify

⁹ p and q are coprimes and a brane (p, q) is identified with a brane $(-p, -q)$

this with the configuration obtained in [33] by starting with $\hat{E}_8, \hat{E}_8, A, A$ (where \hat{E}_8 is the affine version of E_8) and then going down to $\hat{E}_2, \hat{E}_2, A^{16}$. Where $A = X_{[1,0]}$ and \hat{E}_2 will be given below.

The brane assignments in this geometry have been given. If we set the 16 relative local branes to be the A branes, then the non-trivial structure for the branes denoted by $B1\ C2\ C1\ X1$ (and similarly for $B2\ C4\ C3\ X2$) are given by

$$\hat{E}_2 = BCCX_{[3,1]}$$

where $B = X_{[1,-1]}$ and $C = X_{[1,1]}$. This makes clear the notation chosen to denote the branes in Figure 11. In Appendix B we give a review of the properties of the \hat{E}_2 configuration that lead to the identification made.

This assignment of brane type can be replaced by any of its equivalent configurations¹⁰,

$$BCCX_{[3,1]} \sim BCBC \tag{7.2}$$

$$BCCX_{[3,1]} \cong X_{[-1,-1]}X_{[3,1]}X_{[3,1]}X_{[5,1]} \sim CX_{[3,1]}X_{[3,1]}X_{[5,1]} \tag{7.3}$$

where in the first case the branch cut of the $X_{[3,1]}$ brane was moved through the C brane next to it so that it becomes a B on the other side of the C brane. In the second case \cong means a global conjugation by T^2 and after that we used that $X_{[-1,-1]} \sim X_{[1,1]} = C$.

If we compute the monodromy¹¹ around any ordered collection of the branes one finds that it does not have an invariant direction, except when we take the monodromy by the whole group, in which case the monodromy is given by T^8 where T and S are the generators of $SL(2, Z)$. Each of the other 16 branes being of the A type has a T^{-1} monodromy. Therefore, each time the E cycle passes through one of them, the monodromy matrix shifts its power by -1 , until it reaches T^{-8} around the last cycle on the other side. Note the power of monodromy (taking into account orientations) is correlated with the $D8$ brane charge we wish to assign to the orientifold for type I'.

¹⁰ By equivalent we mean that they are related by moving branch cuts. In general, global $SL(2, Z)$ conjugations are also allowed but in our case we restrict the possibilities only to those of the T type since we do not want to change the type of the 16 A branes. See [33] for the general case and more details.

¹¹ Following the conventions of [33], for a configuration of branes $X_{[p_1, q_1]} \dots X_{[p_n, q_n]}$ the total monodromy is given by $K_{[p_n, q_n]} \dots K_{[p_1, q_1]}$

We also discussed the possibility of moving one A brane towards one of the group of 4 branes contained in the last E cycles. Once we do that there is one more possible equivalent configuration given by,

$$ABCCX_{[3,1]} \sim AABX_{[2,1]}X_{[5,1]}$$

It is important to follow the chain of equivalence relations that led to the above result,

$$ABCCX_{[3,1]} \cong ACX_{[3,1]}X_{[3,1]}X_{[5,1]} \sim CX_{[2,1]}X_{[3,1]}X_{[3,1]}X_{[5,1]} \quad (7.4)$$

$$\sim CAX_{[2,1]}X_{[3,1]}X_{[5,1]} \sim AX_{[0,1]}X_{[2,1]}X_{[3,1]}X_{[5,1]} \quad (7.5)$$

$$\sim AX_{[0,1]}AX_{[2,1]}X_{[5,1]} \sim AABX_{[2,1]}X_{[5,1]} \quad (7.6)$$

where in (7.4) \cong is that of (7.3) and \sim is moving A through the C brane becoming an $X_{[2,1]}$ brane. In (7.5) the first \sim is moving the left $X_{[3,1]}$ through $X_{[2,1]}$ becoming an A brane and the second is moving the C through the A becoming a $X_{[0,1]}$ brane. Finally, in (7.6) the first \sim is moving the remaining $X_{[3,1]}$ through $X_{[2,1]}$ becoming an A brane and the last \sim is moving the $X_{[0,1]}$ through the A brane becoming a B brane.

This makes clear that the two A branes in the final result are the same as the two C branes of the initial configuration and that the initial A brane is now a $X_{[2,1]}$ brane.

Let us use this chain to explain the transition between the different Real $K3$'s discussed earlier in this section. Consider in Figure 11 the first A brane approaching $B1$ that according to the result of (7.3) can be thought of as a C brane. These two form an $H_0 = AC$ configuration that has no gauge symmetry associated to it and then take off the real line. This is illustrated in (7.4). Now the $C2$ brane – given by $X_{[3,1]}$ in (7.4) – becomes an A brane in (7.5) and it is free to move in the interval. The remaining four branes still have a total T^8 monodromy. We simply have exchanged one A brane by another A brane. This is the same as exchanging the last brane with its mirror brane in the Type I' language. Now however, we can also push the $C1$ brane pass the $X_{[2,1]}$ monodromy and as before, it converts the $X_{[3,1]}$ brane again to an A brane. This is given in (7.6). Now if we consider the foliation of the E curve to pass just through the $B X_{[2,1]} X_{[5,1]}$ branes, then we obtain the monodromy T^9 . This is again correlated with the charge at the orientifold expected when we pull an extra brane off.

Type I' like descriptions

In the F-theory configuration studied by Sen [24], where the gauge group was $SO(8)^4$, it was possible to show that the Type IIB description was nothing but the orientifold $T^2/(-1)^{F_L} \cdot \Omega \cdot \mathbf{Z}_2$. It was also shown that upon T-duality on each of the circles of the T^2 this orientifold was equivalent to Type I on T^2 . Suppose now that one of the circles of the Type I theory is very small, then we have to go to the T-dual description that is Type I'. Therefore it is natural to expect that the F-theory description in some regimes can be connected to Type I' upon a single T-duality. Of course, this is only possible if on the F-theory side we are working with a configuration that admits a natural S^1 action and in the qualitative analysis we found that this is the case.

In order to study the 9 dimensional limit and get explicit results to match with the Type I' description, we will consider explicit expressions for the metric in the limit corresponding to large eighth radius, and try to get the relevant physical quantities in 9 dimensions.

The crucial point that we will try to argue now is that in the 9 dimensional limit, the generic fiber of the original F-theory compactification is degenerating and moreover the complex structure will grow like $\text{Im}(\tau) \sim R_8$.

In F-theory, as it was pointed out in [3], the middle monomial of $f(z)$ and $g(z)$ will control the complex and kähler structure of the dual heterotic T^2 . In the limit to 9 dimensions both moduli blow up and therefore we expect that the corresponding monomials will dominate the rest at generic points on the z sphere. (See section 8.1 for more details)

This means that in order to get information from the general behavior of the periods of B and E we can consider the elliptic equation to be of the form $y^2 = x^3 + \alpha z^4 x + \beta z^6$. The corresponding periods are obtained, as it was explained in the qualitative part, by integrating the holomorphic 2-form over the corresponding cycle¹².

$$\Gamma_E = \int_E \frac{dx}{y} dz \quad \text{and} \quad \Gamma_B = \int_B \frac{dx}{y} dz$$

rescaling $x \rightarrow z^2 x$ we get the following result,

$$\Gamma_E = \int_a \frac{dx}{\sqrt{x^3 + \alpha x + \beta}} \int_E \frac{dz}{z} = 2\pi i \left(\frac{w_1}{2} \right)$$

¹² Here E and B denote the new elliptic fiber and the new base respectively, but also they are used to denote the projection of the corresponding 2-cycles on the F-theory base.

where the first integral is over the a cycle of the generic fiber of F-theory. This integral is nothing but the first half period $\frac{w_1}{2}$ and the integral over z is independent of the 1-cycle E and gives only $2\pi i$ since the E cycle winds around the origin once.

The period over B is given by

$$\Gamma_B = \int_b \frac{dx}{\sqrt{x^3 + \alpha x + \beta}} \int_B \frac{dz}{z} = \frac{w_2}{2} \ln\left(\frac{z_{X2}}{z_{X1}}\right)$$

where the first integral is over the b cycle and gives us the second half period.

But we know that $\Gamma_E \sim \frac{1}{R_8}$ and $\Gamma_B \sim R_8$. This immediately implies that $w_1 \sim \frac{1}{R_8}$ and $w_2 \ln\left(\frac{z_{X2}}{z_{X1}}\right) \sim R_8$. This tells us that

$$\tau = \frac{w_2}{w_1} \sim R_8$$

at least. But it can not have higher powers of R_8 since τ has to reduce to the heterotic complex structure in the 10 dimensional limit. This implies that $w_2 \sim 1$ and therefore

$$\ln\left(\frac{z_{X2}}{z_{X1}}\right) \sim R_8 \tag{7.7}$$

Now we are ready to continue with the analysis of the limit to 9 dimensions.

The metric for the sphere in the type IIB compactification equivalent to F-theory on $K3$ was given as part of the 10 dimensional metric in (2.32) .

Certainly this metric is very hard to handle under general considerations but here we will make use of some approximations that will become exact in the strict limit to 9-dimensions.

Using that $\text{Im}(\tau) \gg 1$ it is possible to write,

$$\eta(\tau) = q^{1/24} \quad \text{and} \quad q^{-1} = j(\tau) = \frac{f^3}{\Delta} \quad \Rightarrow \quad \frac{\eta^2}{\Delta^{1/12}} = \frac{1}{f^{1/4}} \tag{7.8}$$

Therefore the metric reduces to,

$$ds^2 = k \text{Im}(\tau) \left| \frac{dz}{f^{1/4}(z)} \right|^2$$

This computation only makes sense in the regions where the only monodromies that τ can find are of the form T^n for some integer n . But we saw that this is the case in the regions that we expect to see in the 9 dimensional limit.

Moreover, now we can make use of our knowledge about the zeros of $f(z)$. From Figure 8D we can conclude that in the case where the two branes are real $f(z)$ should have four real zeros inside the minimal cycle of the E class. If the two branes are complex, then we will see in the Appendix B that $f(z)$ still have four zeros (only two of them are real) inside the minimal E cycle even in the case where the latter contains only three branes. Therefore we will have control over $f(z)$ in the 9 dimensional limit when the two minimal E cycles will effectively shrink to a point. The final point we need to work out is the behavior of $\text{Im}(\tau)$.

A very convenient choice of coordinates over the P^1 is one that will parametrize in a natural way the circle action – that become an actual symmetry in the limit – induced by moving along the E class representatives and the position along the B cycle that is the projection of the new P^1 on the F-theory sphere. See Figure 12 and 13.

Let us start by locating the two groups of four branes one near $z = 0$ and the other near $z = \infty$. This means that,

$$|z_i| > \text{Max}(|X1|, |C1|, |C2|, |B1|) \quad |z_i| < \text{Min}(|X2|, |C3|, |C4|, |B2|) \quad (7.9)$$

where we have denoted by z_i with $i = 1, \dots, 16$ the position of the 16 A branes. The branes are ordered by $|z_i| \leq |z_j|$ if $i < j$.

Let $|X1| > \text{Max}(|C1|, |C2|, |B1|)$ and $|X2| < \text{Min}(|C3|, |C4|, |B2|)$, therefore we have, $|X2| \geq |z_{16}| \geq \dots \geq |z_1| \geq |X1|$.

The polynomial $f(z)$ can be written as follows,

$$f(z) = C_2 \prod_{i=1}^4 (z - \hat{z}_i)(z - \hat{\bar{z}}_i)$$

where $|\hat{z}_i| > |X2|$ and $|\hat{\bar{z}}_i| < |X1|$ for all $i = 1, \dots, 4$. If we concentrate in the region $|X1| < |z| < |X2|$ that will be the physical region after the limit, then $f(z)$ can be written approximately as,

$$f(z) = C_2 \left(\prod_{i=1}^4 \hat{z}_i \right) z^4$$

This implies that the metric is roughly $ds^2 \sim \text{Im}(\tau) \left| \frac{dz}{z} \right|^2$, this motivates a conformal transformation from the sphere z to a cylinder by,

$$z = e^w$$

In this new coordinates we can write the discriminant as follows,

$$\Delta = C_1 e^{12(w+w_{cm})} \prod_{i=1}^{24} \sinh\left(\frac{1}{2}(w - w_i)\right)$$

where $w_{cm} = \frac{1}{24} \sum_{i=1}^{24} w_i$ and w_i are the position of the 24 branes in the new coordinates.

From (7.7) we see that the natural coordinates to introduce in order to parametrize the region between $X1$ and $X2$ are $w = R_8(y_1 + iy_2)$ where $y_1, y_2 \in \mathbf{R}$.

Now, in the case where $R_8 \gg 1$ we have that,

$$\sinh\left(\frac{1}{2}(w - w_i)\right) \rightarrow (\text{Phase}) e^{R_8|y_1 - y_1^i|/2}$$

Therefore, the discriminant can be written as,

$$\Delta = C_1 e^{R_8(12(y+y_{cm}) + \frac{1}{2}(y_{x2}+y_{C3}+y_{C4}+y_{B2}) - \frac{1}{2}(y_{x1}+y_{C1}+y_{C2}+y_{B1}) + \frac{1}{2} \sum_{i=1}^{16} |y-y_i|)}$$

In this expression we have replaced $y_1 = \text{Re}(y)$ by y itself in order to save some notation. The C_1 constant contains all the phase factors that were produced in addition to a normalization constant that will be fixed later.

In this coordinates $f(z)$ also takes a special form,

$$f(z) = C_2 e^{R_8(4y + \sum_{i=1}^4 \tilde{y}_i)}$$

Now we are ready to compute $\text{Im}(\tau)$. This can be done by using (2.30).

$$j(\tau) = 1728 \frac{4f^3}{\Delta} = (\text{Phase}) e^{R_8(C_3 + 3 \sum_{i=1}^4 \tilde{y}_i - (y_{x2} + y_{C3} + y_{C4} + y_{B2}) - \frac{1}{2} \sum_{i=1}^{16} y_i - \frac{1}{2} \sum_{i=1}^{16} |y - y_i|)}$$

where C_3 is defined to contain all the constants that might arise from $f(z)$ and Δ . And the factor in front of the exponential contains all the phases from the different terms. This phase factor will not affect $\text{Im}(\tau)$ and reveals the independence of $\text{Im}(\tau)$ from the radial direction of the cylinder.

We will use that $j(\tau) \sim q^{-1}$. This approximation will become exact in the limit $R_8 \rightarrow \infty$ and it is valid in all the regions we are considering, even close to the end points. Now we have to distinguish between the three regimes that were analyzed in previous discussions.

Case I: All 24 branes are real.

Using the above approximation we get that,

$$Im(\tau) = \frac{1}{2\pi} R_8 (C_3 + 3 \sum_{i=1}^4 \tilde{y}_i - (y_{x2} + y_{C3} + y_{C4} + y_{B2}) - \frac{1}{2} \sum_{i=1}^{16} y_i - \frac{1}{2} \sum_{i=1}^{16} |y - y_i|)$$

Now let us use that in the limit, $\tilde{y}_i \sim y_{C3} \sim y_{C4} \sim y_{B2} \sim y_{X2}$ in order to replace all of them by y_{X2} , therefore we get that,

$$Im(\tau) = \frac{1}{2\pi} R_8 \left(C_3 + 8 \left[(y_{X2} - y_{cm}) - \frac{1}{16} \sum_{i=1}^{16} |y - y_i| \right] \right)$$

by the symmetry of the problem, we can always choose $y_{cm} = \frac{1}{16} \sum_{i=1}^{16} y_i$ to be smaller or equal to zero without loss of generality. (This is analog to the freedom of reflecting the interval coordinates in Type I' in order to put the branes as close as possible to the origin).

Now we see that $Im(\tau)|_{(y=y_{X2})} = R_8 C_3$ and $Im(\tau)|_{(y=-y_{X2})} = R_8 (C_3 - 16y_{cm})$ where C_3 has to be fixed by an actual computation of the average of $Im(\tau)$ around the minimal E cycle containing the four branes. This value is controlled by the cross ratio of the four branes positions that is an $SL(2, \mathbf{R})$ invariant and it is the only modulus that survives the limit. This computation tells us that $Im(\tau)$ is positive in the physical region, signalling that our computation is valid.

It is important to notice that the appearance of a piece wise linear function is due to the fact that the logarithmic behavior of the 2 dimensional “electric” potential of the A branes – that are point like charges in the sphere – is smoothed out to a linear function that changes slope at the position of the charge when the limit is taken and the sphere reduces to a 1-dimensional object.

Case II: A pair of branes are complex and 22 branes are real. If we are in the regime of parameters where there are still 4 branes enclosed by the last E curve (on the side where the pair of branes have become complex), then the story is as in case I. However, if the last E curve encloses only three branes, the story changes. Following the same analysis as in case I we get,

$$Im(\tau) = \frac{1}{2\pi} R_8 (C_3 + 3 \sum_{i=1}^4 \tilde{y}_i - (y_{x2} + y_{C3} + y_{C4}) - \frac{1}{2} \sum_{i=0}^{16} y_i - \frac{1}{2} \sum_{i=0}^{16} |y - y_i|)$$

Notice that now the sums run from 0 to 16 since a **new** A brane is in the bulk and its position is denoted by y_0 . The answer in this case is

$$Im(\tau) = \frac{1}{2\pi} R_8 \left(C_3 + 9y_{X2} - \frac{17}{2} y_{cm} - \frac{1}{2} \sum_{i=1}^{16} |y - y_i| \right)$$

Now we see that

$$\text{Im}(\tau) \Big|_{(y=y_{X2})} = R_8(C_3 + \frac{1}{2}y_{X2}) \quad \text{and} \quad \text{Im}(\tau) \Big|_{(y=-y_{X2})} = R_8(C_3 + \frac{1}{2}y_{X2} - \frac{17}{2}y_{cm})$$

In this case the value of C_3 can be fixed completely because we only have three branes inside the minimal cycle and therefore no parameter left after the limit.

Case III: Two pairs of branes are complex and 20 branes are real. Again if the last E curves on either side enclose 4 branes, or one contains 4 and the other 3, we are reduced to cases I and II above. However if the last E curve encloses only 3 branes on each side the story changes. We now have two more ‘visible’ branes in the bulk (whose positions are denoted by y_0 and y_{17}) and the same analysis as above results in

$$\text{Im}(\tau) = \frac{1}{2\pi} R_8(C_3 + 3 \sum_{i=1}^4 \tilde{y}_i - (y_{X2} + y_{C3} + y_{C4}) - \frac{1}{2} \sum_{i=0}^{17} y_i - \frac{1}{2} \sum_{i=0}^{17} |y - y_i|)$$

and using the approximation $\tilde{y}_i \sim y_{C3} \sim y_{C4} \sim y_{X2}$ we get,

$$\text{Im}(\tau) = \frac{1}{2\pi} R_8 \left(C_3 + 9 \left[(y_{X2} - y_{cm}) - \frac{1}{18} \sum_{i=0}^{17} |y - y_i| \right] \right)$$

Now we have that $\text{Im}(\tau) \Big|_{(y=y_{X2})} = R_8 C_3$ and $\text{Im}(\tau) \Big|_{(y=-y_{X2})} = R_8(C_3 - 18y_{cm})$. In this case the two values can be computed. Using the counting of parameters, we can set only 17 positions of the branes to be independent and therefore y_{cm} is frozen to zero. Moreover, as discussed in Case II, the value of $\text{Im}(\tau)$ at the ends is also frozen since we only have three branes and no cross ratio can be constructed, hence, no modulus survives the limit.

The computation of the constant C_3 can be done explicitly in the Cases II and III, since all we have to do is to choose a configuration where the three branes are isolated and compute $\text{Im}(\tau)$ as they collapse to a point. The configuration we are talking about is called $\hat{\hat{E}}_0$ [35] [33] and it is known to be out of the reach of Kodaira singularities at finite distance in moduli space in 8 dimensions. However, the limit to 9 dimensions is at infinite distance and the collapse to a point becomes meaningful. In the appendix A it is shown that following the analysis of [35] the $\hat{\hat{E}}_0$ configuration can be properly isolated and the value we are looking for is given by $\text{Im}(\tau) = \frac{1}{2}$.

In Case II, this implies that $R_8(C_3 + \frac{1}{2}y_{X2}) = \frac{1}{2}$ and in Case III we get that $R_8(C_3) = \frac{1}{2}$.

Therefore, in the limit to 9 dimensions we get in the first case that $C_3 + \frac{1}{2}y_{X2} \rightarrow 0$ and in the second $C_3 \rightarrow 0$ since they go as $\frac{1}{R_8}$.

Summarizing the results of this part, we have found that the metric in each case is given by

$$ds^2 = k \text{Im}(\tau) \left| \frac{dz}{z} \right|^2 + \eta_{\mu\nu} dx^\mu dx^\nu = k R_8^2 \text{Im}(\tau) (dy_1^2 + dy_2^2) + \eta_{\mu\nu} dx^\mu dx^\nu$$

where k is an overall constant that is the usual F-theory - heterotic duality contains information about the 8-dimensional heterotic coupling since the latter is related to the overall volume of the P^1 base. And $\text{Im}(\tau)$ is given by,

$$\text{Im}(\tau) = \begin{cases} \frac{1}{2\pi} R_8 \left(C_3 + 8 \left[(y_{X2} - y_{cm}) - \frac{1}{16} \sum_{i=1}^{16} |y - y_i| \right] \right) & \text{Case I} \\ \frac{1}{2\pi} R_8 \left(\frac{17}{2} \left[y_{X2} - y_{cm} - \frac{1}{17} \sum_{i=1}^{16} |y - y_i| \right] \right) & \text{Case II} \\ \frac{1}{2\pi} R_8 \left(9 \left[y_{X2} - \frac{1}{18} \sum_{i=0}^{17} |y - y_i| \right] \right) & \text{Case III} \end{cases}$$

Up to terms of order 0 in R_8 that will become irrelevant in the limit $R_8 \rightarrow \infty$

Connection to Type I' and Type I' like descriptions

Now we are ready to find the connection of our descriptions to Type I' in the case where we expect Type I' to be valid using the observation made from Sen's analysis.

In the coordinates for the cylinder we find that the 10 dimensional metric is given by

$$ds^2 = k R_8^2 \text{Im}(\tau) (dy_1^2 + dy_2^2) + \eta_{\mu\nu} dx^\mu dx^\nu$$

where $\mu, \nu = 0, \dots, 7$. (Here we are back to the notation $y = y_1 + iy_2$)

This metric is in the Einstein frame. This is the frame where the $SL(2, \mathbf{Z})$ U-duality group of IIB theory is manifest.

The idea is to perform a T-duality along the circles that the limit to 9-dimensions has created for us. Therefore, we first have to go to the string frame by using that $G^{(E)} = e^{-\frac{\phi_{\text{IIB}}}{2}} G^{(S)}$. By definition $\text{Im}(\tau) = e^{-\phi_{\text{IIB}}}$ and therefore we get,

$$ds_{(s)}^2 = k R_8^2 (\text{Im}(\tau))^{1/2} (dy_1^2 + dy_2^2) + (\text{Im}(\tau))^{-1/2} (\eta_{\mu\nu} dx^\mu dx^\nu) \quad (7.10)$$

In the decompactification limit, the y_2 dependence of $\text{Im}(\tau)$ drops out as it was shown before. This makes manifest that the circle action predicted in the qualitative part has become exact.

Before performing the T-duality we should give make k a bit more explicit. k can be computed – as we will do in the $E_8 \times E_8$ example – by the fact that the volume of the P^1 of F-Theory should be equal to the heterotic coupling in 8 dimensions.

The volume is easy to compute since the metric is just a cylinder with varying radius in y_1 . Therefore, using the metric we have,

$$\text{Vol}(P^1) = 2\pi k R_8 \int_{-y_{x2}}^{y_{x2}} F(y) dy$$

where we have defined $F(y) = \frac{2\pi \text{Im}(\tau)}{R_8}$. Therefore the integral is finite in the limit $R_8 \rightarrow \infty$.

Using now that $\text{Vol}(P^1) = e^{\phi_{hs}}$ and that $e^{\phi_{hs}} = \frac{e^{\phi_{h(10)}}}{(R_9 R_8)^{1/2}}$ we get that the singular behavior of k is $k \sim R_8^{-5/2}$. This result tells us that the metric (7.10) behaves as follows,

$$ds^2 \sim F(y_1)^{1/2} (dy_1^2 + dy_2^2) + R_8^{-1/2} F(y_1)^{-1/2} (\eta_{\mu\nu} dx^\mu dx^\nu)$$

Let us now perform the T-duality in the 8-th direction. This will only change the radius of the 8-th circle to its inverse. Remember that $y_2 \sim y_2 + \frac{2\pi}{R_8}$. Introducing a new variable x^8 and rescaling the other x^μ the metric can be written schematically as follows,

$$ds^2 = F(y_1)^{1/2} dy_1^2 + F(y_1)^{-1/2} (\eta_{\mu\nu} dx^\mu dx^\nu)$$

where now $\mu, \nu = 0, \dots, 8$.

Finally, we would like to bring the metric to a conformally flat metric. This can be done by a simple change of coordinates since the metric only depends on y_1 and it is already in the desired form in 9 of the dimensions. The change of coordinates will have to be such that,

$$F(y_1)^{1/2} dy_1^2 = F(y_1)^{-1/2} dx_9^2 \quad (7.11)$$

Once this is done the metric looks like $ds^2 = F(y_1)^{-1/2} (\eta_{MN} dx^M dx^N)$ where $(M, N = 0, \dots, 9)$.

The final step is to express $F(y)$ in terms of x_9 . The result of doing this is simply that, up to a constant¹³,

$$F(y) = (z(x_9))^{2/3}$$

¹³ In a more detailed computation, as will be done for some examples in section 8.1, all the constants that we have not written can be computed and reproduces precisely the results expected from Type I'.

where $z(x_9)$ are the functions in (2.5) for the case with 24 real branes and a generalization like (5.3) for the case with 20 real branes.

For the example of 8.2 we will be able to compute all the relevant quantities of Type I' from this description, i.e., B , C and the position of the branes.

The other computation that can be done explicitly is the appearance of the dilaton of Type I' as the T-dual of the IIB dilaton.

Here we only need to use that the T-dual IIB dilaton $\tilde{\phi}$ is given by,

$$e^{\tilde{\phi}} = \mathcal{R} e^{\phi_{IIB}} \quad (7.12)$$

where the dual radius \mathcal{R} is given by $F(y)^{-1/4} R_8$. But $e^{\phi_{IIB}} = (\text{Im}(\tau))^{-1} = R_8^{-1} F(y)^{-1}$. Therefore we get,

$$e^{\tilde{\phi}} = F(y)^{-5/4} = (z(x_9))^{-5/6}$$

that is precisely the behavior expected in Type I' as was shown in in (2.6).

8. EXAMPLES

In this section we first review the 9 dimensional limit of $E_8 \times E_8$ theory by taking the appropriate limit of F-theory. We then show how the real resolution of $E_8 \times E_8$ gives rise to the real $K3$ structure anticipated on general grounds.

8.1. 9 dimensional limit of $E_8 \times E_8$

In the quantitative analysis of section 7 we described how the connection between Real $K3$ configurations and Type I' like descriptions can be achieved. It is the aim of this part of the section to apply all the result we got to a simple case where we expect the usual Type I' description and to show how non trivial quantities match with full precision. The point we are going to study is the $E_8 \times E_8$. The relevant Type I' description was given in section 2.1 with the important results at the end of the section.

We will start by considering the 8 dimensional description of the $E_8 \times E_8$ theory with zero Wilson lines in terms of F-theory.

The moduli space of the heterotic compactification is given in terms of two complex parameters, U denoting the complex structure and T denoting the complexified Kähler structure of the T^2 , and one real parameter given by the 8 dimensional coupling constant.

The F-theory model in this case is given in terms of the following elliptic equation,

$$y^2 = x^3 + \alpha z^4 x + z^5(1 + \beta z + z^2) \quad (8.1)$$

The defining polynomials are $f(z) = \alpha z^4$ and $g(z) = z^5(1 + \beta z + z^2)$. α and β are complex parameters that should be mapped to the U and T and the volume of the P^1 base will be related to the heterotic coupling constant.

The explicit map was found in [25] and it is given by

$$j(iU)j(iT) = -1728^2 \left(\frac{\alpha}{3}\right)^3 \quad (8.2)$$

$$(j(iU) - 1728)(j(iT) - 1728) = 1728^2 \left(\frac{\beta}{2}\right)^2 \quad (8.3)$$

In (8.2) we can see that the $(\text{PSL}(2, Z) \times \text{PSL}(2, Z))/Z_2$ symmetry of the heterotic compactification is explicit in the map.

Now let us take the decompactification limit on the heterotic side, this means that we are taking a rectangular ($\theta = 0$) torus with zero B-field ($B_{12} = 0$) and $R_8^h \gg R_9^h > R_{9c}^h$. With this choice we are breaking the full $(\text{PSL}(2, Z) \times \text{PSL}(2, Z))/Z_2$ symmetry but at the end we will recover the Z_2 symmetry of the S^1 heterotic compactification to 9 dimensions.

In this limit, we can approximate $j(iU) = e^{2\pi U}$ and $j(iT) = e^{2\pi T}$.

The discriminant of (8.1) is given by

$$\Delta = 4f^3 + 27g^2 = z^{10} (4\alpha^3 z^2 + (1 + \beta z + z^2)^2) \quad (8.4)$$

The roots of (8.4) can easily be found by noting that (8.4) can be factorized in two quadratic pieces,

$$\Delta = 27z^{10} \left(z^2 + \left(\beta + 2 \left(-\frac{\alpha}{3} \right)^{3/2} \right) z + 1 \right) \left(z^2 + \left(\beta - 2 \left(-\frac{\alpha}{3} \right)^{3/2} \right) z + 1 \right) \quad (8.5)$$

Using the map (8.2) we find that in the limit the roots behave as follows,

$$z_1 = e^{-\pi(T-U)} \quad z_2 = e^{\pi(T-U)} \quad z_{X1} = -e^{-\pi(T+U)} \quad z_{X2} = -e^{\pi(T+U)} \quad (8.6)$$

It is important to notice that the four roots came out real, two on R^+ and two on R^- while the E_8 singularities are located at $z = 0$ and at $z = \infty$.

We can also obtain these results directly from our discussion of the relation between the periods of the base and elliptic fiber and the radius of the eighth dimension derived in (6.3). The periods we are interested in can be written in the following form,

$$\Gamma = \int_{\gamma} |p - \tau q| \left| \frac{\eta^2(\tau)}{\Delta^{1/12}} \right| |dz| \quad (8.7)$$

where γ is the relevant 1-cycle on the F-theory P^1 base shown in Figure 12. This formula for the periods is the same that would give the mass of a (p, q) BPS open string stretched along γ . It is possible to choose basis in which $X1$ and $X2$ are $(3, 1)$ branes and z_1 and z_2 are $(1, 0)$.

Here we will only assume that $Im(\tau) \gg 1$. This implies that the period formula reduces to,

$$\Gamma = \int_{\gamma} |p - \tau q| |\alpha|^{-1/4} \left| \frac{dz}{z} \right| \quad (8.8)$$

It is possible to remove the $|\alpha|^{1/4}$ factor since it is an overall normalization of the periods and we will be computing only ratios. Let us compute first the period corresponding to $\gamma = E$ and the cycle $(1, 0)$,

$$\mathcal{E}_8 = \int_{|z|=1} \left| \frac{dz}{z} \right| = 2\pi \quad (8.9)$$

Next, let us compute the period corresponding to $\gamma = B$ and the cycle $(1, 0)$,

$$\mathcal{B}_9 = \int_{z_1}^{z_2} \left| \frac{dz}{z} \right| = 2\ln(z_2) \quad (8.10)$$

where we have been done of the fact that $z_1 = 1/z_2$. From the heterotic string we learn that the ratio of these to periods should be equal to $T - U$.

This immediately tells us that,

$$\frac{\mathcal{B}_9}{\mathcal{E}_8} = T - U = \frac{\ln(z_2)}{\pi} \Rightarrow z_2 = e^{\pi(T-U)} \quad (8.11)$$

In order to compute z_{X1} we need the value of τ and following a procedure similar to that of the previous section we get,

$$\tau = \frac{i}{2\pi} (3\ln(\alpha) - \ln(z_{X2}) - \ln(z_2)) \quad (8.12)$$

From the elliptic equation we have that we can choose $z_2 \in \mathbf{R}^+$ and $z_{X2} \in \mathbf{R}^-$ and $\alpha \in \mathbf{R}^-$.

This implies that $|\tau| = \frac{1}{2\pi} \ln \left(\frac{\alpha^3}{z_{X2} z_2} \right)$. Now we can compute the two other periods corresponding to $\gamma = E$ and the cycle $(3, 1)$ and to $\gamma = B$ and the cycle $(3, 1)$,

$$\mathcal{E}_9 = \int_{|z|=1} |\tau| \left| \frac{dz}{z} \right| = \ln \left(\frac{\alpha^3}{z_{X2} z_2} \right) \quad (8.13)$$

Finally, after a some computations,

$$\mathcal{B}_8 = \int_{z_{X1}}^{z_{X2}} |\tau| \left| \frac{dz}{z} \right| = \frac{1}{2\pi} (2 \ln(-z_{X2}) \ln(-\alpha^3) - 3 \ln^2(-z_{X1}) - \ln^2(z_2)) \quad (8.14)$$

Using the ratio $\mathcal{E}_9/\mathcal{E}_8 = U$ it follows from (8.9) , (8.13) and (8.11) that,

$$\frac{\alpha^3}{z_{X2}} = e^{\pi(T+U)} \quad (8.15)$$

The last independent ratio we have is,

$$\frac{\mathcal{B}_8}{\mathcal{E}_8} = TU \quad (8.16)$$

Using (8.11) , (8.15) and (8.16) we get our final result,

$$z_{X2} = -e^{\pi(T+U)} \quad z_1 = e^{\pi(T-U)} \quad (8.17)$$

It is important to remark that the periods for this example can also be computed explicitly without the use of the 9-dimensional limit in terms of hypergeometric functions [36] , but in this example we were interested in showing how the approximation works and become exact in the limit in a simple case. We have thus found perfect agreement with the results of [25].

The metric on the P^1 is given by (2.32). Let us restrict our attention to the region of the P^1 given by $\Gamma = \{z \in C \mid e^{-\pi(T+U)} < |z| < e^{\pi(T+U)}\}$. It is not hard to check that $|j(\tau)| \gg 1 \quad \forall \quad z \in \Gamma$. This justifies the use of the approximations of all the previous sections and we write the metric as,

$$ds^2 = k(Im(\tau)) |\alpha|^{-1/2} \left| \frac{dz}{z} \right|^2 \quad (8.18)$$

If τ were constant, this metric would describe a cylinder, so it is natural to change coordinates given by the conformal map from the complex plane to a cylinder of radius

2π , namely, $z = e^w$ as it was suggested in the previous section. Now we introduce $w = R_8(y_1 + iy_2)$. In the notation of the previous section we have,

$$y_{X2} = \pi(R_9 + \frac{2}{R_9}) \quad y_9 = \pi(R_9 - \frac{2}{R_9}) \quad y_8 = -y_9 \quad y_{X1} = -y_{X2}$$

Now we can compute $\text{Im}(\tau)$ with the following result,

$$\text{Im}(\tau) = \frac{R_8}{2\pi} [y_{X2} - \frac{1}{2}|y + y_9| - \frac{1}{2}|y - y_9|]$$

This is already looking like the structure in (2.18) .

Next we have to compute the volume of the F-theory sphere in this limit. This is easily done using the metric at hand and integrating only on the region between $-y_{X2}$ and y_{X2} . The result is given by,

$$\text{Vol}(P^1) = 8\pi^2 k R_8^2 |\alpha|^{-1/2}$$

using that $\text{Vol}(P^1) = e^{\phi_{h8}} = \frac{e^{\phi_{h10}}}{(R_8 R_9)^{1/2}}$ we can compute k explicitly with the following result,

$$k = \frac{1}{8\pi^2} e^{\phi_{h10}} |\alpha|^{1/2} R_8^{-5/2} R_9^{-1/2}$$

The metric (8.18) that is in the Einstein frame is finally given by,

$$ds^2 = \frac{1}{8\pi^2} e^{\phi_{h10}} R_8^{-1/2} R_9^{-1/2} \text{Im}(\tau) (dy_1^2 + dy_2^2)$$

The next step is to go to the string frame, but for this we have to consider the full 10 dimensional metric that is given in (2.32).

We want to make explicit all the R_8 dependence, therefore let us define $F(y) = \frac{2\pi}{R_8} \text{Im}(\tau)$ and $y_2 = R_8 \theta$ so that $\theta \sim \theta + 2\pi$. And the result is given by,

$$ds^2 = \frac{e^{\phi_h}}{R_9^{1/2}} F(y)^{1/2} (dy_1^2 + R_8^{-2} d\theta^2) + R_8^{-1/2} F(y)^{-1/2} (\eta_{\mu\nu} dx^\mu dx^\nu)$$

At this point we should expect to be able to get some of the results of section 2.1, in particular, we can compute the proper distances from y_9 to y_{X2} and from $-y_9$ to y_9 .

Let us start with y_9 to y_{X2} ,

$$\Phi_1 = \int_{y_9}^{y_{X2}} \sqrt{G_{99}(y)} dy = \frac{\lambda_h^{1/2}}{R^{3/2}}$$

The second proper distance is given by,

$$\Phi_2 = \int_{-y_9}^{y_9} \sqrt{G_{99}(y)} dy = \lambda_h^{1/2} \frac{(R^2 - 2)}{R^{3/2}}$$

Remembering that in the map (8.2) and (8.3) we are working with $E_8 \times E_8$ variables we find that we have been able to reproduce (2.25) and (2.26) solely from F-theory.

Now we are ready to perform a T-duality in the θ direction and now it is clear that this direction is going to be non compact in the limit $R_8 \rightarrow \infty$, therefore we introduce x^8 and by some finite rescalings that do not depend on y_1 we can write the metric as follows,

$$ds^2 = \frac{e^{\phi_h}}{R_9^{1/2}} \left[F(y_1)^{1/2} dy_1^2 + \gamma^2 F(y_1)^{-1/2} (\eta_{\mu\nu} dx^\mu dx^\nu) \right] \quad (8.19)$$

where γ is a generic constant that can be used to fix the range of the only compact coordinate left. Note that this does not affect the proper distances we computed earlier.

Finally we would like to bring the metric to the conformal gauge by defining $F(y_1)^{1/2} dy_1 = \gamma dx_9$. Imposing that $y_1 = -y_{X2}$ implies $x = 0$ and that $y_1 = y_{X2}$ corresponds to $x = 2\pi$ we can fix the integration constant and γ .

Now, if we define $x = x_1$ to correspond to $y = -y_9$ we get that,

$$x_1 = 2\pi \frac{4}{(3R_9^2 + 2)}$$

and this is exactly the expression found in (2.21).

The metric now can be written as,

$$ds^2 = \frac{\lambda_h}{R^{1/2}} \gamma^2 F(y(x))^{-1/2} (\eta_{MN} dx^M dx^N)$$

but it turns out that $F(y(x)) = \gamma^{2/3} z(x)^{2/3}$ and $\gamma = R^{-3/2} (3R^2 + 2)$, therefore we get for the metric the following,

$$ds^2 = \lambda_h \frac{(3R^2 + 2)^{5/3}}{R^3} z(x)^{-1/3} (\eta_{MN} dx^M dx^N)$$

this is again in agreement with (2.24).

Finally we want to compute the dual of the IIB coupling. According to (7.12), we only need to compute the dual radius, i.e., the radius of the 8-th direction after the T-duality. This radius can be read off from (8.19) and it is given by $\mathcal{R} = \frac{R^{1/4}}{\lambda^{1/2}} F(y)^{-1/4} R_8$.

Using (7.12) and that $e^{\phi_{II}} = (\text{Im}(\tau))^{-1} = R_8^{-1} F(y)^{-1}$ and the expression of $F(y)$ in terms of x we get the following for the dual coupling,

$$e^{\tilde{\phi}} = \lambda^{-1/2} R^{3/2} (3R^2 + 2)^{-5/6} z(x)^{-5/6}$$

that reproduces (2.23).

Therefore we see that we have been able to recover all aspects of the Type I' description in 9 dimensions by taking the decompactification limit of F-theory from 8 dimensions.

8.2. “Real Resolution of $E_8 \times E_8$ ”

Up to now we have shown that the real $K3$ encoding the 9 dimensional heterotic behavior consists of a Riemann surface of genus 10 and a sphere. This was done by using tools of real algebraic geometry. It is the aim of this part to show how the Real $K3$ mentioned before arises directly from a full resolution of the $E_8 \times E_8$ point by turning on “real” Wilson lines on the heterotic side. This means that we are turning on only the Wilson lines in the 9-th direction.

In order to go ahead in spite of not having the explicit map between the Wilson lines and the coefficients of the polynomials of the elliptic equation we will take the following strategy. We will start with the point in the heterotic $E_8 \times E_8$ where all Wilson lines are zero. The map in this case is known explicitly. The next step is a resolution from $E_8 \rightarrow E_7$ on both singularities, in this case the number of parameters is still small and the deformations are uniquely determined. Beyond this point the global analysis of the $K3$ is not possible at least with the techniques we have at hand. Therefore we perform a local analysis of each of the E_7 singularities. The small resolutions are achieved via the invariant theory for Weyl groups as was done in [37].

Global analysis

Let us start with the $E_8 \times E_8$ point on the F-theory side. Using $SL(2, C)$ we can set one E_8 singularity at $z = 0$. This means using table 2 that,

$$f(z) = a_4 z^4 + \dots + a_8 z^8 \quad g(z) = b_5 z^5 + \dots + b_{12} z^{12} \quad (8.20)$$

It is also possible to set the other E_8 at $z = \infty$ and therefore we should impose,

$$f(z) = a_4 z^4 \quad g(z) = b_5 z^5 + b_6 z^6 + b_7 z^7 \quad (8.21)$$

This is obtained by changing variables $z = 1/w$ and using the global rescaling invariance of the elliptic equation.

Now we can use our last $SL(2, C)$ degree of freedom by a rescaling of z in order to make $b_5 = b_7 = b$, and finally we use the global rescaling of the elliptic equation¹⁴ to set $b = 1$.

This gives us the $E_8 \times E_8$ polynomials to be,

$$f(z) = \alpha z^4 \quad g(z) = z^5(1 + \beta z + z^2) \quad (8.22)$$

¹⁴ The rescaling is given by $y \rightarrow \lambda^3 y$, $x \rightarrow \lambda^2 x$, $f \rightarrow \lambda^4 f$, $g \rightarrow \lambda^6 g$

The resolution to $E_7 \times E_7$ can only affect the f polynomial since the condition on the order of g is the same for E_7 as that for E_8 . We have to lower the order by one unit of the zeros of f at the location of the E singularities. This gives us,

$$f(z) = z^3(a_1 + \alpha z + a_2 z^2) \quad g(z) = z^5(1 + \beta z + z^2) \quad (8.23)$$

Local analysis

Any ADE singularity on an elliptic $K3$ can be modeled locally by means of an ALE space. The ALE spaces can be thought of as algebraic varieties in C^3 given by the following equations,

Type	ALE singularity
A_n	$xy + z^{n+1} = 0$
D_n	$x^2 + yz^2 - z^{n+1} = 0$
E_6	$-x^2 - xy^2 + y^3 = 0$
E_7	$-x^2 - y^3 + 16yz^3 = 0$
E_8	$-x^2 + y^3 - z^5 = 0$

Table 3: Equations in C^3 defining ALE spaces with the singularity located at the origin.

The key idea in the resolution using the Cartan generators is to realize that the coefficients in the deforming polynomials should be generators of the algebra of polynomials invariant under the Weyl group of the corresponding root system.

As an example we will consider the A_n case. Here we will follow [37] closely and the details of the other cases can be found there.

Let e_i $i = 1, \dots, n+1$ be orthonormal basis of R^{n+1} , then the root system of A_n is generated by the following set of simple roots $v_i = e_i - e_{i+1}$. We define a set of distinguished functionals t_1, \dots, t_{n+1} given by,

$$t_i = -v_{i-1}^* + v_i^* \quad (1 \leq i \leq n+1) \quad (8.24)$$

where v_i^* are the dual of the root basis.

In this case we have to consider the Weyl group of A_n that is nothing but the symmetric or permutation group S_{n+1} . Therefore the basis of invariant polynomials of t_i can be obtained by considering the coefficients of the following auxiliary polynomial,

$$P(U) = \prod_{i=1}^{n+1} (U + t_i) = U^{n+1} + \sum_{i=1}^{n+1} s_i U^{n+1-i} \quad (8.25)$$

This is the way to define the i -th symmetric functions $s_i = s_i(t_1 \dots t_{n+1})$ that are in this case the basis we were looking for.

Now the resolution of the A_n singularity can be achieved by the following deformations of the expression in Table 3:

$$xy + P(z) = 0 \quad (8.26)$$

Going back to our case, we are interested in the resolutions of E_7 . It turns out that the deformation takes the form [37] ,

$$-y^2 - x^3 + 16xz^3 + \varepsilon_2 x^2 z + \varepsilon_6 x^2 + \varepsilon_8 xz + \varepsilon_{10} z^2 + \varepsilon_{12} x + \varepsilon_{14} z + \varepsilon_{18} = 0 \quad (8.27)$$

where ε_i are the basis of the algebra of polynomials invariant under the Weyl group action of E_7 and are given as functions of s_1, \dots, s_7 . For the explicit form of the ε_i see Appendix 2 of [37].

The E_7 ALE singularity has the same structure as an elliptic equation, therefore we can easily read off the $f(z)$ and $g(z)$ after the appropriate changes of variables. The answer is given by,

$$f(z) = -16z^3 - \frac{1}{2}\varepsilon_2^2 z^2 - \left(\frac{2}{3}\varepsilon_2\varepsilon_6 + \varepsilon_8\right)z - \frac{1}{3}\varepsilon_6^2 - \varepsilon_{12} \quad (8.28)$$

$$g(z) = \frac{16}{3}\varepsilon_2 z^4 + \left(\frac{2}{27}\varepsilon_2^3 + \frac{16}{3}\varepsilon_6\right)z^3 + (\varepsilon_{10} + \frac{2}{9}\varepsilon_6\varepsilon_2^2 + \frac{1}{3}\varepsilon_8\varepsilon_2)z^2 + \left(\frac{2}{9}\varepsilon_6^2\varepsilon_2 + \varepsilon_{14} + \frac{1}{3}\varepsilon_{12}\varepsilon_2 + \frac{1}{3}\varepsilon_8\varepsilon_6\right)z + \left(\frac{2}{27}\varepsilon_6^3 + \frac{1}{3}\varepsilon_{12}\varepsilon_6 + \varepsilon_{18}\right) \quad (8.29)$$

Our next step is clearly to perform a full resolution of the E_7 singularity. We will see with an example that choosing a generic “real” Wilson line, i.e., real t_i ’s, we get that the surface has three holes and no spheres. Together with the global analysis this means that the total smooth space consists of a Riemann surface of genus 10 and a sphere.

Let us try now to consider examples where we can illustrate all the transitions between the different regimes discussed in section 7 and the different embeddings of some groups in the real $K3$. Let us consider the following family of deformations $(t_1, \dots, t_7) = (-1, 1, \dots, t)$. This correspond to the following elliptic equation,

$$f(z) = -16z^3 - \frac{1}{3}(784 + 592t + 136t^2)z^2 - 24(27 + t)(t + 2)^2 z - 27(t + 2)^4 \quad (8.30)$$

$$g(z) = \left(\frac{448}{3} + \frac{128}{3}t + 16t^2\right)z^4 + \frac{1}{9}\left(\frac{49088}{3} + 18304t + 7184t^2 + \frac{2752}{3}t^3\right)z^3 + 8(25t^2 + 130t + 196)(t + 2)^2 z^2 + 72(2t + 7)(t + 2)^4 z + 54(t + 2)^6 \quad (8.31)$$

The discriminant is given by,

$$\Delta = z^5(-16384z^4 + a(t)z^3 + b(t)z^2 + 2304(35t^4 + 182t^3 + 119t^2 - 372t - 36)(t+2)^2z + 41472(t+3)(t-1)t(t+2)^4) \quad (8.32)$$

It is easy to see that there is always an A_4 singularity at $z = 0$ but it becomes A_5 at $t = 0$ and $t = 1$. Less evident is that at $t = -1$ we get instead of A_5 an extra A_1 singularity. Finally we see that at $t = 2$ we get a D_5 singularity.

The transitions are shown in Figures 14 and 15 with the corresponding Dynkin Diagram of E_7 showing the unbroken piece for each value of t .

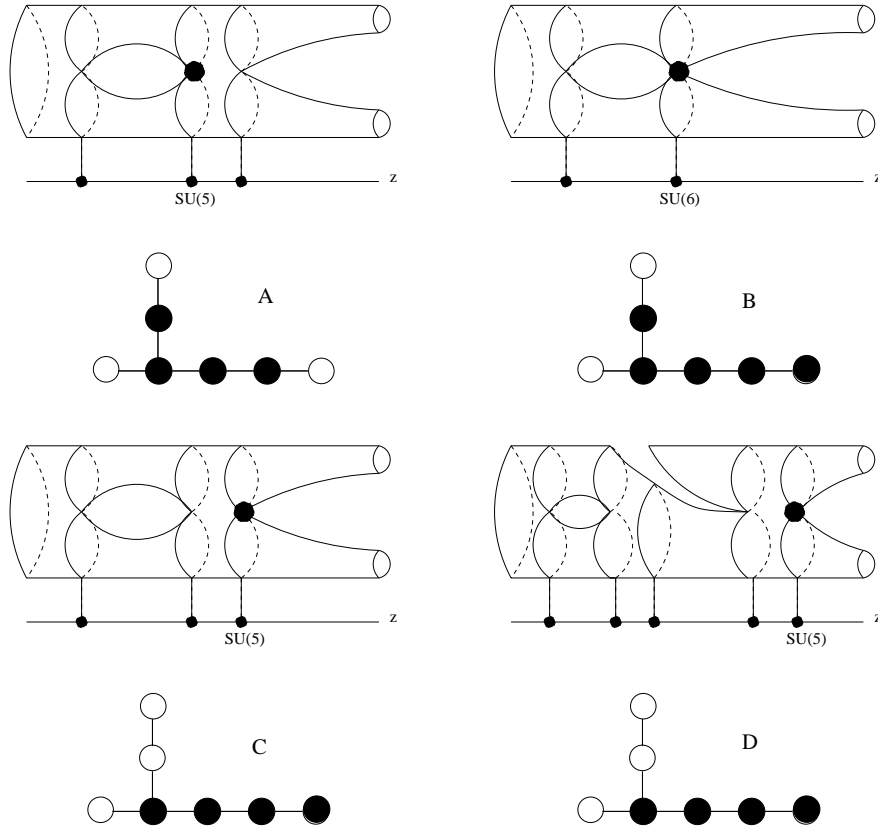


Figure 14: One parameter family of Real resolutions of E_7 showing the transition when two branes become real (C-D) and embeddings of $SU(5)$ and $SU(6)$ in E_7

In Figure 14A we see that the $SU(5)$ is embedded in the way corresponding to the non-trivial value for the Z_2 Wilson line. In Figure 14B the brane at the right joined the $SU(5)$ to give an $SU(6)$ gauge group. In Figure 14C one of the original branes in the $SU(5)$ separates from the $SU(6)$ giving again $SU(5)$ but with a different embedding. In Figure 14D we see the result after the two branes that were complex land on the real axis without

modifying the gauge group. In Figure 15A one of the new branes joins the $SU(5)$ group to give an $SU(6)$ with the embedding corresponding to the trivial choice of Z_2 Wilson line. In Figure 15B one of the branes separates to the left leaving an $SU(5)$ again with the trivial Z_2 Wilson line. In Figure 15C the two branes to the left of the “Hook” join to give an extra $SU(2)$. Finally we see that when the $SU(5)$ branes, the “Hook” and one of the two branes of the left side join we get an $SO(10)$ gauge group.

Even though this family cannot show it, if we start from Figure 14B it is possible to get the final brane on the left to join the group in order to give an $SU(7)$. This $SU(7)$ is one of the groups that requires one “extra” brane from the view point of Type I’ since the Type I’ description of E_7 involves only 6 D8-branes at the orientifold with infinite coupling.

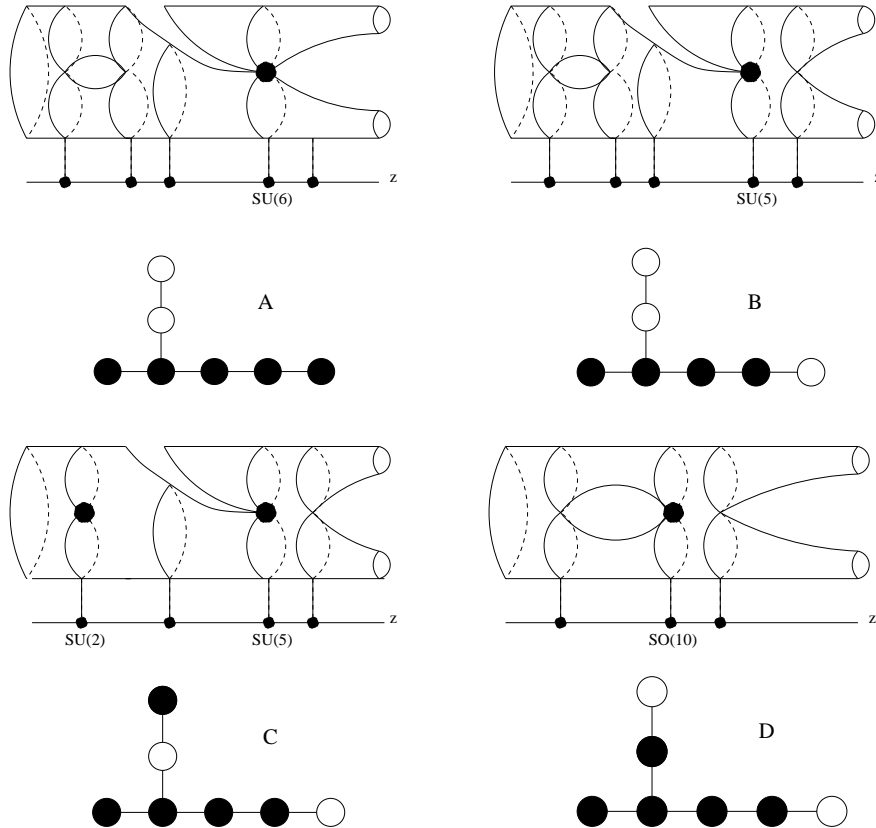


Figure 15: Embeddings of $SU(6)$, $SU(5)$, $SU(5) \times SU(2)$ and $SO(10)$ in E_7 .

Acknowledgements:

We would like to thank D. Allcock, O. Bergman, A. Chari, K. Hori, J. Maldacena, D. Morrison, T. Pantev, S. Sinha, A. Strominger and B. Zwiebach for valuable discussions.

The research of F.C. was supported by a fellowship from CONICIT and Universidad Simón Bolívar. The research of C.V. is partially supported by NSF grant PHY-98-02709.

Appendix A. Map between the heterotic theories at the $E_8 \times E_8$ point

In section 2.1 we described the $E_8 \times E_8$ point of the heterotic $SO(32)$ as an enhancement of the $SO(14) \times SO(14)$ point. This description led to a Type I' scenario with infinite coupling at both orientifolds. However, as mentioned in section 2.1 this point is most naturally described in term of heterotic $E_8 \times E_8$ variables and the map between them is the aim of this appendix.

The moduli in the $E_8 \times E_8$ theory consists of the 9 dimensional radius R_{E8} and the 10 dimensional coupling λ_{E8} . The Wilson lines are all zero. On the other hand, the moduli in the $SO(32)$ theory consists of the radius R_{SO} , the coupling λ_{SO} and the Wilson lines are $\theta_I = (0^7, \frac{1}{2} - \lambda, \lambda, \frac{1}{2})^7$ where λ and R_{SO} are related by

$$R_{SO}^2 = 2\lambda(\frac{1}{2} - \lambda) \quad (\text{A.1})$$

The way to map the two theories at more complicated points than the one we are discussing is to find the $SO(17, 1)$ rotation that connects them. For an example interpolating between the two theories see [29].

Here however, due to the fact that R_{SO} should be given only in terms of R_{E8} , a single relation will be enough. In particular, we can compare the masses of the BPS states responsible for the extra $SU(2)$ enhancement of symmetry in both theories and then get the map.

On the $E_8 \times E_8$ theory, the $SU(2)$ is achieved at the critical radius and therefore the new states should be the usual states of winding and momentum number ± 1 and neutral with respect to the $E_8 \times E_8$.

The mass is given by ¹⁵

$$M_{BPS}^2 = P_R^2 = \left(\frac{1}{R_{E8}} - \frac{R_{E8}}{2} \right)^2$$

As we expect, the mass is zero at the critical radius for zero Wilson lines $R_{E8}^2 = 2$

On the $SO(32)$ theory, the states becoming massless at the $SU(2)$ point are just off diagonal vector bosons of the original $SO(32)$ group with charges (or root vectors) $P = \pm(e_8 - e_9)$ where e_i are orthonormal vectors in R^{16} where the root system lives. This states have no winding or momentum. Using the mass formula,

$$M_{BPS}^2 = R_R^2 = \left(\frac{\theta_I P_I}{R_{SO}} \right)^2 = \frac{4}{R_{SO}^2} \left(\lambda - \frac{1}{4} \right)^2$$

¹⁵ Setting $\alpha' = 2$

Here we are summing over I . We see that for $\lambda = \frac{1}{4}$ these states are massless as we expect.

Finally, using (A.1) in order to express everything in terms of R_{SO} and then equating the two masses we get,

$$R_{SO}^2 = \frac{R_{E8}^2}{4(1 + R_{E8}^2)^2}$$

Now it is possible to find the relation between the two coupling constants in 10 dimensions. This is achieved by equating the couplings in 9 dimensions and using that in S^1 compactifications $\lambda_9^2 = \frac{\lambda_{10}^2}{R}$.

The result given in terms only of R_{E8} is,

$$\lambda_{E8} = (R_{E8}^2 + 2)^{1/2} \lambda_{SO}$$

Appendix B. Description of \hat{E}_2

The aim of this appendix is to show the computation that was used in section 7 for the value of $\text{Im}(\tau)$ at the location of the three branes left inside the minimal E cycle.

It was shown in [35] [38] that the configurations of branes given by \hat{E}_n ($1 \leq n \leq 8$), $\hat{\tilde{E}}_0, \hat{\tilde{E}}_1$ can be properly isolated. This means that there exists polynomials¹⁶ $f(z)$ and $g(z)$ such that the relevant branes are around $z = 0$ and the others are at $z = \infty$.

Let us consider the two parameter family of polynomials giving the properly isolated $\hat{E}_2, \hat{\tilde{E}}_1, \hat{\tilde{E}}_1$ and $\hat{\tilde{E}}_0$.

The family is given by [35] [38],

$$f(z) = z^4 + z^3 + \frac{1}{4}sz^2 + \frac{1}{16}tz \quad (\text{B.1})$$

$$g(z) = z^6 + \frac{3}{2}z^5 + \frac{3}{8}(1+s)z^4 + \frac{1}{32}(3t+6s-1)z^3 + \frac{3}{128}(1-2s+s^2+2t)z^2 \quad (\text{B.2})$$

$$-\frac{3}{256}(s-1)(s-t-1)z + \frac{(14+18s^2-2s^3+12t+3t^2-6s(5+2t))}{2048} \quad (\text{B.3})$$

For generic (t, s) we have an \hat{E}_2 configuration. The discriminant given by $\Delta = -f^3 + g^2$, is a polynomial of degree five and the coefficient of z^5 term is given by,

$$(-2 + 2s - t)(3 - 4s + s^2 + t) \quad (\text{B.4})$$

¹⁶ Here we will use the definition of [35] for $f(z)$ and $g(z)$ where the discriminant is $\Delta = -f^3 + g^2$ and not $\Delta = 4f^3 + 27g^2$ as we were using in the rest of this work.

revealing the existence of two branches. It is also important to mention that the discriminant has an overall factor of $(s - 1)$ signaling that $s = 1$ is at infinite distance away in the moduli space. In figure 16A we show $K3_R$ around the five branes of \hat{E}_2 .

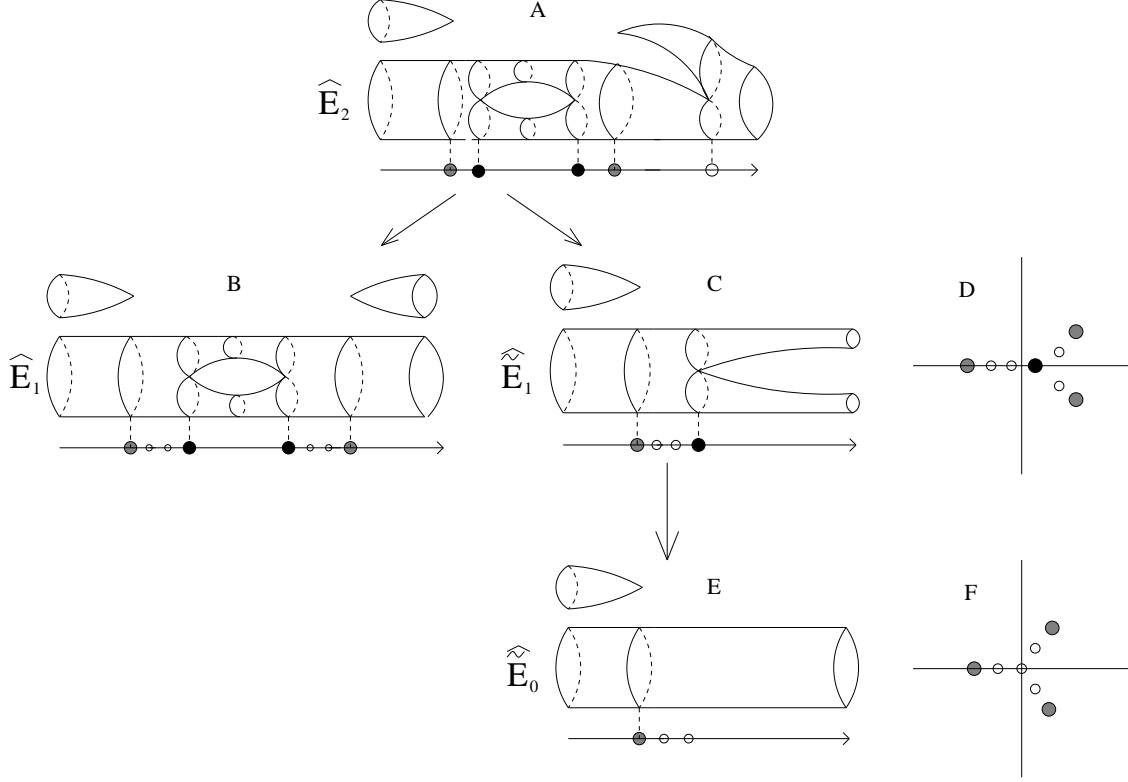


Figure 16: $K3_R$ in the vicinity of brane configurations \hat{E}_2 , \hat{E}_1 , $\hat{\hat{E}}_1$ and $\hat{\hat{E}}_0$. Besides the $\hat{\hat{E}}_1$ and $\hat{\hat{E}}_0$ also the locations of the branes and zeros of $f(z)$ (small white dots) are shown in the complex z -plane.

The first branch $t = 2(s - 1)$ gives the \hat{E}_1 configuration. The region in the s line we are interested in is given by $1 < s < -\frac{1}{2} + \sqrt{3}$. The lower bound is the one discussed before, and the upper bound is an $SU(2)$ wall. In figure 16B we show how $K3_R$ looks like around the four real branes of \hat{E}_1 after the A brane of \hat{E}_2 has escaped to infinity. We see that the two branes that form the $SU(2)$ are $C1$ and $C2$ of section 7. It is also possible to check that $f(z)$ has four real zeros indicated by small white dots in figure 16B.

The second branch $t = -3 + 4s - s^2 = (s - 1)(3 - s)$ gives $\hat{\hat{E}}_1$. In this case, the brane A and B come off the real line and the branes $C2$ escapes to infinity. The resulting $K3_R$ around the remaining two branes on the real axis is shown in figure 16C. The region of s is given by $1 < s < \frac{3}{2}$. The upper bound comes from the z^4 coefficient of the discriminant

that vanishes at $s = \frac{3}{2}$ signaling that the $C1$ brane moves all the way to infinity leaving us with a $\hat{\tilde{E}}_0$ configuration.

Finally the $\hat{\tilde{E}}_0$ configuration has no parameters left since we have set $s = \frac{3}{2}$. It is possible to see that upon a shift in z and a rescaling, the discriminant (a cubic) for this configuration is given by $z^3 - 1$ and $f(z) = z(z^3 - \frac{8}{9})$ (See figure 16D). This shows the statement made in section 7 about the zeros of $f(z)$ being enclosed by the last E cycle.

The fact that the $\hat{\tilde{E}}_0$ has a Z_3 symmetry tells us that in the limit to 9 dimensions in which the E cycle shrinks to a point this configuration will collapse to $z = 0$. The effect of the limit and of the remaining branes can only affect this configuration in a global z rescaling or a rescaling of $f(z)$ and $g(z)$ given before. But none of them affects the value of $j(\tau)$ at $z = 0$ that always vanishes since $f(z = 0) = 0$ and $\Delta(z = 0) \neq 0$. This implies that

$$\tau|_{(z=0)} = \frac{\sqrt{3}}{2} + i\frac{1}{2}$$

From this we can get the result we were looking for the computation of the boundary values of $\text{Im}(\tau)$ in the Case II and Case III of the quantitative part of section 7, namely, $\text{Im}(\tau) = \frac{1}{2}$.

References

- [1] E. Witten, “String Theory Dynamics In Various Dimensions,” [hep-th/9503124](#) Nucl. Phys. B443 (1995) 85-126
- [2] C. Vafa, “Evidence for F-Theory,” [hep-th/9602022](#), Nucl. Phys. B469 (1996) 403-418
- [3] D. Morrison and C. Vafa, “Compactifications of F-Theory on Calabi-Yau Threefolds – I,II,” [hep-th/9603161](#), [9603161](#), Nucl. Phys. B473 (1996) 74-92, Nucl. Phys. B476 (1996) 437-469
- [4] A. Kumar and C. Vafa, “U-Manifolds,” [hep-th/9611007](#), Phys. Lett. B396 (1997) 85-90
- [5] K.Narain, M. Sarmadi and C. Vafa, “Asymmetric Orbifolds,” Nucl. Phys. B 288 (1987) 551
- [6] A. Dabholkar and J. A. Harvey, “String Islands,” [hep-th/9809122](#)
- [7] E. Witten, “Toroidal Compactification Without Vector Structure,” [hep-th/9712028](#), JHEP 9802 (1998) 006
- [8] M. Bershadsky, T. Pantev and V. Sadov, “F-theory with quantized fluxes,” [hep-th/9805056](#)
- [9] S. Kachru, A. Klemm and Y. Oz, “Calabi-Yau Duals for CHL Strings,” [hep-th/9712035](#), Nucl.Phys. B521 (1998) 58-70
- [10] T. Banks, W. Fischler and L. Motl, “Duality versus Singularities,” [hep-th/9811194](#), JHEP 9901 (1999) 019
- [11] S. Kachru and C. Vafa, “Exact Results for N=2 Compactifications of Heterotic Strings,” [hep-th/9505105](#), Nucl. Phys. B450 (1995) 69-89
- [12] S. Ferrara, J. A. Harvey, A. Strominger and C. Vafa, “Second-Quantized Mirror Symmetry,” [hep-th/9505162](#), Phys.Lett. B361 (1995) 59-65
- [13] A. Klemm, W. Lerche and P. Mayr, “K3 – Fibrations and heterotic-Type II String Duality,” [hep-th/9506091](#), Phys. Lett. B357 (1995) 313-322
- [14] C. Vafa and E. Witten, “Dual String Pairs With N=1 And N=2 Supersymmetry In Four Dimensions,” [hep-th/9507050](#), Nucl. Phys. Proc. Suppl. 46 (1996) 225-247
- [15] S.Hosono, B.H.Lian and S.-T.Yau, “ Calabi-Yau Varieties and Pencils of K3 Surfaces,” [alg-geom/9603020](#)
- [16] J. Polchinski and E. Witten, “Evidence for heterotic-Type I String Duality,” [hep-th/9510169](#), Nucl. Phys. B460 (1996) 525-540
- [17] D. Morrison and N. Seiberg, “Extremal Transitions and Five-Dimensional Supersymmetric Field Theories,” [hep-th/9609070](#), Nucl. Phys. B483 (1997) 229-247
- [18] P. Horava and E. Witten, “heterotic and Type I String Dynamics from Eleven Dimensions,” [hep-th/9510209](#), Nucl. Phys. B460 (1996) 506-524 and “Eleven-Dimensional Supergravity on a Manifold with Boundary”,[hep-th/9603142](#), Nucl. Phys. B475 (1996) 94-114

- [19] K.S.Narain, “New heterotic Theories in Uncompactified Dimensions < 10 ,” Phys. Lett. 169B,41 (1986). K.S.Narain, M.H.Sarmadi, and E. Witten, “A Note on Toroidal Compactification of heterotic String Theory,” Nucl. Phys.B 279. J.P. Serre, A course in Arithmetic (Springer, Berlin, 1973)
- [20] O. Bergman, M. Gaberdiel and G. Lifschytz, “String Creation and heterotic-Type I’ Duality,” hep-th/9711098, Nucl. Phys. B524 (1998) 524-544
- [21] C. Bachas, M. Green and A. Schwimmer, “(8,0) Quantum mechanics and symmetry enhancements in type I’ superstrings,” hep-th/9712086, JHEP 9801 (1998) 006
- [22] J. Polchinski, S. Chaudhuri and C. Johnson, “Notes on D-Branes,” hep-th/9602052
- [23] B.R.Greene, A. Shapere, C. Vafa and S.-T. Yau, “Stringy Cosmic Strings and Non-compact Calabi-Yau Manifolds,” Nucl. Phys. B337 (1990) 1
- [24] A. Sen, “F-Theory and Orientifolds,” hep-th/9605150, Nucl. Phys. B475 (1996) 562-578
- [25] G. Cardoso, G. Curio, D. Lüst and T. Mohaupt, “On The Duality Between The heterotic String and F-Theory in 8 Dimensions,” hep-th/9609111, Phys. Lett. B389 (1996) 479-484
- [26] N. Seiberg, “Five Dimensional SUSY Field Theories, Non-trivial Fixed Points and String Dynamics,” hep-th/9608111, Phys. Lett. B388 (1996) 753-760
- [27] M. Douglas, S. Katz and C. Vafa, “Small Instantons, del Pezzo Surfaces and Type I’ theory,” 9609071, Nucl. Phys. B497 (1997) 155-172
- [28] D. Allcock, private communication.
- [29] P. Ginsparg, “On Toroidal Compactification of Heterotic Superstrings,” Phys. Rev. D35 (1987) 648-654
- [30] T. Mohaupt, “Critical Wilson Lines in Toroidal Compactifications of Heterotic Strings,” Int. J. Mod. Phys. A8 (1993) 3529-3552
- [31] P. Aspinwall, “Enhanced Gauge Symmetries and $K3$ Surfaces,” hep-th/9507012
- [32] V. Nikulin, in *Proc. Int. Congress of Mathematicians*, University of California, Berkeley, 1986, p. 654.
- [33] O. De Wolfe, T. Hauer, A. Iqbal and B. Zwiebach, “Uncovering the Symmetries on $[p, q]$ 7-branes: Beyond the Kodaira Classification”, hep-th/9812028. “Uncovering Infinite Symmetries on $[p, q]$ 7-branes: Kac-Moody Algebras and Beyond”, hep-th/9812209
- [34] P. Aspinwall, “M-Theory Versus F-Theory Pictures of the Heterotic String,” hep-th/9707014, Adv. Theor. Math. Phys. 1 (1998) 127-147
- [35] A. Sen and B. Zwiebach, “Stable Non-BPS States in F-theory,” hep-th/9907164
- [36] W. Lerche and S. Stieberger, “Prepotential, Mirror Map and F-Theory on $K3$,” hep-th/9804176, Adv. Theor. Math. Phys. 2 (1998) 1105-1140
- [37] S. Katz and D.R. Morrison, “Gorenstein Threefold Singularities with Small Resolutions Via Invariant Theory for Weyl Groups,” Jour. Alg. Geom. 1 (1992) 449
- [38] Y. Yamada and S.K. Yang, “Affine 7-brane Backgrounds and Five-Dimensional E_N Theories on S^1 ,” hep-th/9907134